Electrochemical detection of 2,6-diisopropylphenol

RACKUS, DARIUS,GEORGE

DURHAM UNIVERSITY

ELECTROCHEMICAL DETECTION OF 2,6-DIISOPROPYLPHENOL

Darius G. Rackus, M. Sci.

November 2011

Submitted in Partial Fulfilment of the degree of
Master of Science in Chemistry
Chemistry Department
Durham University

ABSTRACT

Propofol is a general anæsthetic used for long-term sedation. Currently, propofol is administered intravenously and dosage is determined by patient weight. In rare cases, patients under long-term treatment can develop propofol infusion syndrome, which may result in death. While sensitive, current detection methods for plasma concentrations of propofol are too slow. Faster detection methods for point of care testing need to be developed, and electrochemical methods may be the solution. Various electrochemical methods for the detection of propofol are explored. Detection by facilitated transport at the interface between two immiscible electrolyte solutions is shown to have potential as a detection method. Various chemically modified glassy carbon electrodes are also explored for propofol detection. A sensor for propofol was not developed, but this exploratory study suggests that an electrode modified by a combination of carbon nanotubes and methylene blue may prove to be an effective sensor.

TABLE OF CONTENTS

LIST OF FIGURES

GLOSSARY OF TERMS

Term	Meaning
ACN	Acetonitrile
CA	Chronoamperometry
CE	Counter Electrode
CME	Chemically Modified Electrode
CNT	Carbon Nanotube
CV	Cyclic Voltammetry
DCE	1,2-dichloroethane
DPV	Differential Pulse Voltammetry
E	Potentential/Voltage
GCE	Glassy Carbon Electrode
HPLC	High Performance Liquid Chromatography
i	Current
ITIES	Interface between Two Immiscible Electrolyte Solutions
MB	Methylene Blue
MIP	Molecularly Imprinted Polymer
MWNT	Multiwall Carbon Nanotube
NaPβCD	Phosphated β-Cyclodextrin Sodium Salt
PEDOT	Poly-3,4-ethylenedioxythiophene
PRIS	Propofol Infusion Syndrome
RE	Reference Electrode
SPCE	Screen Printed Carbon Electrode
SWNT	Single-Wall Carbon Nanotube
SWV	Square Wave Voltammetry
TBACl	Tetrabutylammonium chloride

TBATPB	Tetrabutylammonium tetraphenylborate
TCI	Target Controlled Infusion
WE	Working Electrode
$\boldsymbol{\nu}$	Scan rate
$\boldsymbol{\Delta G^{0,w\rightarrow o}_{transfer,i}}$	Gibbs energy of transfer
$\boldsymbol{\Delta^w_o \phi^0_i}$	Standard potential of transfer
μITIES	Micro Interface between Two Immiscible Electrolyte Solutions

ACKNOWLEDGEMENTS

Above all, I would like to thank my God and Father for His provision for me and for the way He sustains me through all things, even this testing thesis.

I would also like to thank my supervisor, Dr Ritu Kataky for taking me on as a student, securing funding for this project, and most importantly for her constant guidance throughout this work.

Thanks must also go to my labmates and friends, Rui Campos, Paula Lopes, Alice Delcourt-Lançon, and Rachel Daunton. Your help, your time, and your friendship has been extremely valuable over this past year. Thank you to Drs Paul Chazot and Anil Suri for being sounding boards when times got tough.

Lastly, I must thank my parents for putting up with yet one more year of my living overseas. Thank you for your support and love in all my years.

CHAPTER 1 : LITERATURE REVIEW

INTRODUCTION

Propofol (2,6-diisopropylphenol) is a general anæsthetic used for both the induction and the maintenance of anæsthesia. Rapid onset and reversibility of sedation has led to propofol as a popular sedative so that it is commonly administered to patients under intensive care.[1] Unfortunately, adverse effects are known to be associated with the administration of propofol, referred to as propofol infusion syndrome (PRIS). PRIS is strongly associated with a high dosage over an extended period of time (>4 mg kg^{-1} hr^{-1}, 48 hr), and has a high mortality rate. Currently, the mechanism of PRIS remains unknown and no treatment has been established.[2,3]

Currently, propofol is administered based on various patient parameters, as determined by pharmacokinetic and pharmacodynamic modelling.[4] Computer operated target controlled infusion (TCI) pumps are commonly used and several models exist which administer propofol based on patient age, height, sex, and body weight. There are many physiological factors which these models cannot account for, and, so accuracy is limited, particularly in children and elderly patients.[5] Therefore, there is a need for timely and accurate measurements of propofol plasma concentration that can be coupled with TCI systems for more accurate and safer administration of propofol.

Progress is being made towards point-of-care testing for propofol. This review will briefly cover the chemical background of propofol before examining the analytical methods already developed for propofol detection. This will provide a context for the work laid out in this thesis.

CHEMICAL BACKGROUND

Propofol is a double substituted phenol with two isopropyl groups situated *ortho* to the hydroxyl group and has a molecular weight of 178.27 g mol^{-1} (see Fig. 1.1). It is a tan-yellow oil at room temperature, but freezes at 18 °C.

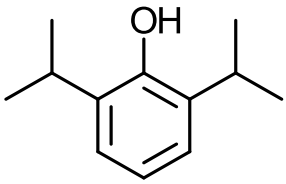

Fig. 1.1 Chemical structure of propofol.

Propofol is highly lipophilic (logP=4.16), accounted for by its benzene ring and isopropyl side chains. The hydroxyl group is weakly ionisable with a reported pK_a of 11. As a result, propofol is not very water soluble and has a miscibility of 150 μg L^{-1} (841 μM).[1]

Because of its highly lipophilic nature, propofol is administered as an emulsion. The most common, Diprivan®, is available as a 1 or 2% propofol emulsion with 10% soybean oil, 1.2% lecithin, and EDTA as an antimicrobial additive.[1,6]

DETECTION METHODS

Chromatographic methods

The most common analytical method employed to evaluate plasma concentrations of propofol is separation by high performance liquid chromatography (HPLC) coupled with various different detectors. Detection methods include fluorimetric assays,[7] derivatisation followed by colorimetric detection,[8] and electrochemical detection.[9,10]

Fluorimetric assays

Fluorometric detection of propofol is relatively straightforward. It is a technique used throughout the literature whereby, after separation, propofol is detected by excitation at 276 nm and emission at 310 nm after separation by HPLC.[7,11] Quantification requires the use of an internal standard by which to compare the signal corresponding to propofol. Chromatograms showing propofol and an internal standard are given below in Fig. 1.2. Interference of propofol metabolites can be eliminated through extraction by cyclohexane. Improvements to the technique really only come by modifications to the sample preparation step, as this is the most tedious and time consuming, taking at least 30 min.[11]

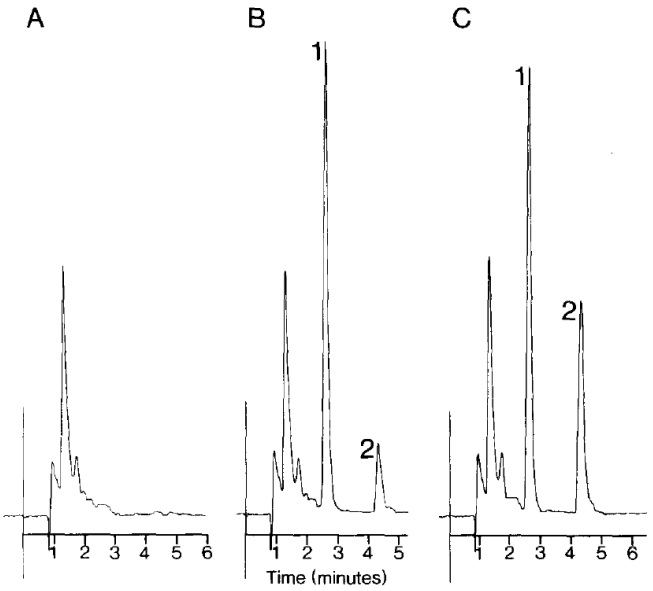

Fig. 1.2 Chromatograms of blood samples with (A) as a control, (B) spiked with propofol, and (C) propofol as administered to a patient. Peak 1 is the internal standard thymol and peak 2 is propofol. Taken from Plummer[7], with permission.

Colorimetric detection

Propofol in and of itself absorbs in the UV at 276 nm. However, it has a low molar absorptivity, rendering direct UV detection ineffective at clinically relevant levels.[8] Derivatisation with Gibbs reagent can be used to enhance the molar absorptivity.

The presence of phenols can be detected and quantified using Gibbs' method, which was originally described in 1927.[12] Quinonechloroimides react with para-unsubstituted phenols to produce quinoneimine dyes. The reaction with propofol under basic conditions, which results in a rich blue indophenol, is given below in Fig. 1.3.

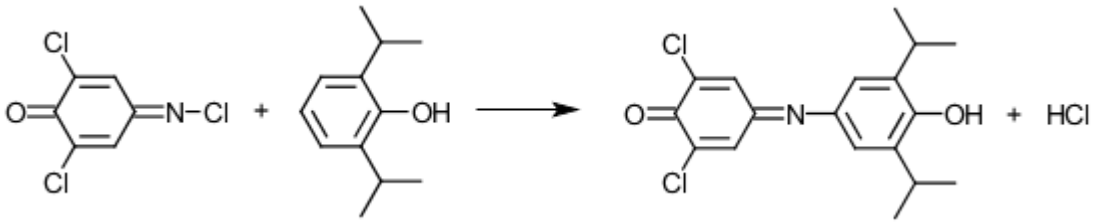

Fig. 1.3 Reaction of 2,6-dichloroquione-4-chloroimide with propofol under to produce a quinoneimine and hydrochloric acid.

The blue dye rapidly converts to a colourless form under the acidic conditions and has a higher absorbance at 276 nm. The indolphenol is not stable and has a decomposition half-life of approximately 30 min.[8] Combined with HPLC, a detection limit of 25 ng ml^{-1} (1.4×10^{-7} M) is achievable.

Electrochemical detection

Despite the relative ease and advantages electrochemical detection methods offer, there has been very little written on the electrochemical detection of propofol. However, the electrochemical detection of other phenols, most notably Δ^9-tetrahydrocannabinol (the

active ingredient in cannabis) has been achieved by adapting the Gibbs reaction. For work on blood or serum, electrochemical methods, to date, are dependent on chromatographic separation techniques.[9,10]

An early instance of coupling electrochemical detection with chromatography was reported by Uebel *et al.* In this work, porous in-line graphite electrodes were coupled with column chromatography. Detection was in amperometric mode, with the two electrodes held at constant potentials, one for the oxidation of propofol and one for the oxidation of the internal standard. The method required an internal standard, and was comparable to other detection techniques, with a limit of detection of 80 ng ml^{-1} (4.48×10^{-7} M).[9] Although not as sensitive as fluorimetric detection techniques, this method shows the advantages and ease of electrochemical detection. Coupling with chromatography, however, still requires extensive sample preparation.

Further work coupling electrochemical detection with chromatographic separation has led to increased sensitivities. Like other phenolic compounds, propofol has been shown to oxidise at a lower potential under alkaline conditions. As the pH of the solution is raised above the pK_a of propofol, the phenolic proton is lost. The propofol anion thus, has a lower oxidation potential. Additionally, in reversed phase HPLC, ionic species elute faster than non-ionic species.[10]

Pissinis *et al.* were able to show that propofol, like other phenolic compounds, will polymerise upon oxidation.[10,13] This can be detected by CV with an oxidation peak for propofol on the forward scan and the appearance of a second oxidation peak at a lower potential indicative of the polymer (or dimer) product during subsequent scans. This is

shown in Fig. 1.4. Repetitive cycling leads to fouling of the electrode with a propofol polymer that is adsorbed to the electrode surface.[10,14]

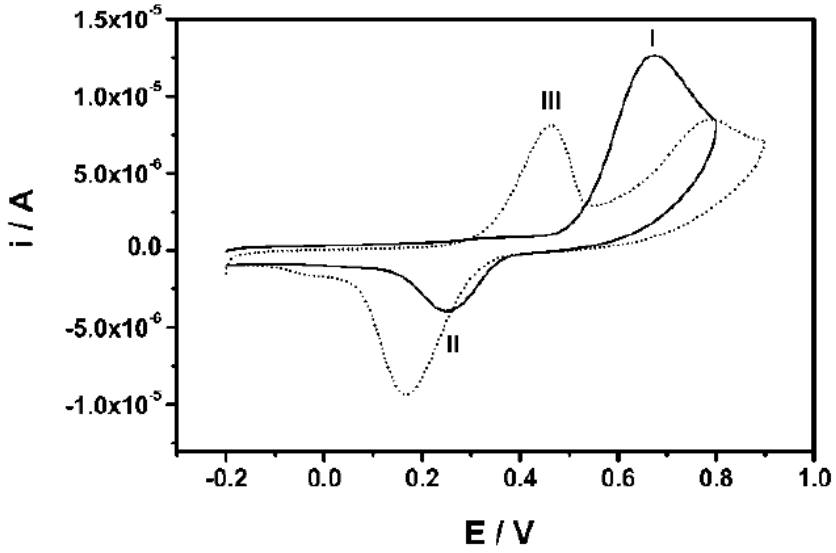

Fig. 1.4 CV response of 500 µM propofol in a buffer-ACN mixture (90:10 v/v) at pH 3. Scan rate 40 mV s^{-1}. Peak I is indicative of propofol oxidation, whereas peak III corresponds to the oxidation of the propofol dimer. Taken from Pissinis *et al*. (2007)[10], with permission.

When coupled with chromatographic separation, electrochemical detection is a powerful and accurate technique. However, this is a method that still requires trained personnel, expensive equipment, and most importantly time. Time is actually the most important parameter to consider in testing, given that a bolus injection of propofol sedates a patient for 4-6 min, but quantification by HPLC takes at least 5 min.[15] Point of care testing, requiring minimal or no sample preparation, thus, is an attractive goal, and electrochemical methods are currently being developed for such use.[14,16]

Interfering species in blood necessitates sample preparation or a means of increasing selectivity and reducing fouling. An alternative approach is to sample other body fluids, such as urine. Thiagarajan *et al*.[16] have shown that propofol can be measured in urine by using pre-anodised screen printed carbon electrodes (SPCE). SPCE can be anodized by

repetitive cycling in 0.5 M H_2SO_4 solution. The pre-anodisation modifies the electrode surface by oxidising it, introducing carbonyl, carboxylic, and hydroxyl functional groups. This oxidised surface offers a catalytic advantage in oxidising propofol, and has been shown to aid in discrimination between dopamine, ascorbic acid, and uric acid—interfering species expected in urine. This method has a reported detection limit of 8×10^{-8} M, which is still higher than detection limits achieved with chromatographic separations.[16]

One of the largest concerns with electrochemical detection of propofol, as previously mentioned, is the formation a polymeric layer that can foul the electrode surface.[10,14] Costetin *et al*.[17] suggest that the electrochemical dimerization of phenols in aqueous solvents proceeds in a concerted manner. That is, both proton and electron transfer occur in the same step. In conjunction with cathodic stripping voltammetry, the product of propofol oxidation can be related to the concentration of propofol in a solution. Rather than measuring the concentration of propofol in solution, the reduction of the oxidised product is used. This occurs at a potential where the effect of interfering species should be limited. However, this technique is not consistently reproducible.[14]

Another concern regarding the electrochemical detection of propofol is the orientation of adsorbed phenol on the electrode surface. Phenols have been shown to change orientation on gold surfaces in a voltage dependent manner. At lower potentials, phenols lay flat along the electrode surface and are bonded through their π-system. At higher potentials, they orientate themselves in a vertical manner and can bond covalently through the lone pair of the oxygen atom.[18] This becomes a concern because bonding energy will affect the coulometric charge required to strip off the adsorbate.[19]

Alternatively, Langmaier *et al*.[14] have suggested limiting the potential window of the working electrode for better detection of propofol. The reason being that as the product of propofol oxidation is reduced, it adsorbs more strongly to the electrode surface. Avoiding the potential at which the oxidation product is reduced prevents the film from obstructing the signal corresponding to propofol that has not been oxidised.[14,20]

Currently, the literature does not contain any means of directly measuring the concentration of propofol in blood by electrochemical means.

Gas phase detection

Because of the volatility of propofol, it can be detected in exhaled breath.[21] It is estimated that the levels of propofol in expired breath are of the order of parts-per-billion.[21] This has proven to be an attractive approach for measuring patient propofol levels. The majority of methods utilise mass spectrometry,[22-25] while optical detection for gas phase detection has recently been developed.[21] Optical detection methods are simpler than separation and quantification by gas chromatography and mass spectrometry, and have the potential of being incorporated into small devices for use at a patient's bedside. The challenge with optical detection in the gas phase comes from interfering species, particularly acetone, water, and CO_2. Laurila *et al*.[21] have shown that, using a photoacoustic setup, propofol can be measured between 260-280 nm, where possible interfering species are not detected. This technique can achieve detection limits of 0.12 ± 0.22 ppb.[21]

Molecularly imprinted polymers

Molecularly imprinted polymers (MIPs) are a promising means for propofol detection and devices have been developed that use this technology for clinical measurements.

MIPs have been described as artificial antibodies due to their ability to discriminate between molecules. Unlike antibodies which require aqueous working environments and an optimal pH, MIPs do not. MIPs are created by mixing monomer and a desired analyte together. Polymerisation is then induced and usually involves crosslinking agents. What results is a polymer structure laced with the analyte. An extraction of the analyte leaves a polymer with cavities specific to the shape of the analyte. The polymer is then exposed to a solution containing the desired analyte, where it binds to the cavities.[15,26] The polymer can then be moved to another solution where the analyte is extracted and then measured, as described in Fig. 1.5.

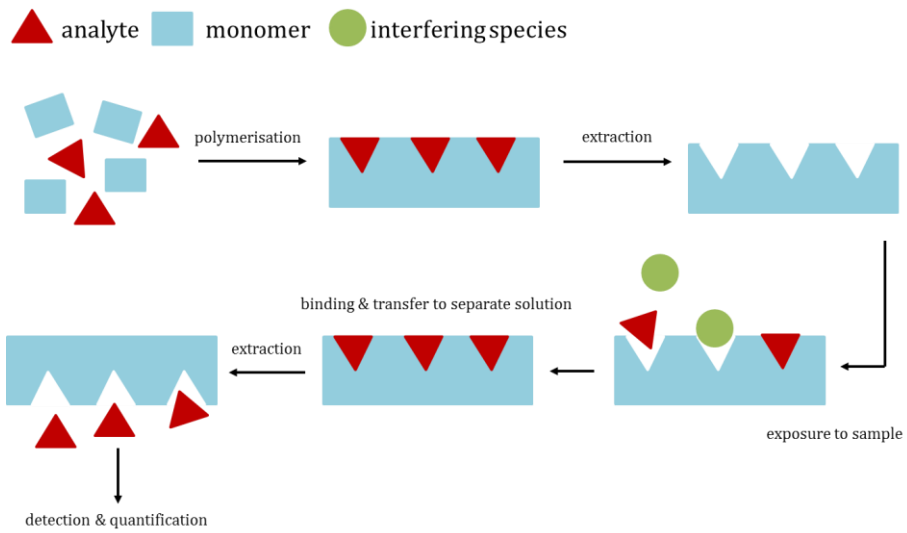

Fig. 1.5 Preparation of a MIP and its use in detection.

MIPs for propofol detection have been developed and studied by Miruna Petcu, and MIPs are now being employed by different groups for propofol detection. Petcu *et al.*[24] developed MIPs using propofol or the derivative propofol (4-vinylphenyl) carbonate. Covalent imprinted polymers were prepared using the propofol derivative, which had to be hydrolysed prior to extraction. These MIPs offered very low cross-reactivity in the presence of cresols and exhibited non-specific binding of 2%, both desirable traits for a sensor.[26]

When MIPs are synthesised on a support such as a membrane or glass, they can be controlled in terms of surface area and shape. This can lead to an increase in selectivity and sensitivity. Coupled with colorimetric tests (*i.e.* Gibbs reagent), propofol can be detected in blood samples down to concentrations between 0 and 2 μg ml^{-1}.[15] MIPs prepared on cyclic olefin copolymer have been used to create a biochip for propofol detection. The olefin copolymer offers the advantage that it is transparent so optical detection of propofol can be done through the substrate and MIP layer. When coupled with a microfluidic setup, automation can be achieved, although the same steps of loading the MIP with the analyte, removing the sample, and exposing the MIP to Gibbs reagent are still required.[27]

The use of MIPs in sensing is not restricted to colorimetric tests, such as Gibbs reagent, but can also be coupled with electrochemical methods. Electropolymers such as poly-(3,4-ethylenedioxythiophene) (PEDOT) are ideal as the MIP can be prepared directly on an electrode through eleyctropolymerisation. PEDOT alone has been shown to increase the sensitivity of amperometric sensors for morphine by acting as a catalyst for morphine oxidation. When formed into a MIP, this catalytic advantage is combined with the selectivity afforded by the MIP. Even in the presence of the structurally related molecule codeine, which differs from morphine by an OH/MeO, PEDOT MIPs are able to selectively bind morphine.[28]

MIP coated gold electrodes for the detection of propofol have also been developed, but unfortunately do not show the desired benefits as expected from MIP based sensors. The introduction of a MIP layer to a gold electrode has been shown to decrease the amperometric signal 10-fold. Additionally, the problem of electrode fouling is not

eliminated by the use of MIPs.[29] This renders MIPs still unsuitable for in-flow analysis applications.

CONCLUSIONS

The detection methods of propofol that have been reviewed here have been summarised in Table 1.1. The clinically relevant range for propofol detection is 5-50 $\times 10^{-6}$ M. All the detection methods have limits that fall within that range, yet there is not a technique fast enough to provide results in real-time for a point-of-care situation.

Table 1.1 Summary of propofol detection methods

	Method	Detection Sample	Limit of Detection	Ref.
1	HPLC + Gibbs Reagent	Blood	1.4×10^{-7} M	[8]
2	HPLC + Fluorometric	Blood	1.1×10^{-8} M	[7]
3	HPLC + Electrochemical	Blood	4.5×10^{-7} M	[9]
4	Photoacoustic Spectroscopy	Gas	0.12 ppb	[219]
5	Preanodised SPCE	Urine	8×10^{-8} M	[16]
6	Carbon Electrodes a)Stripping Voltammetry b)Limited Potential Window	Lab Sample	 3.2×10^{-6} M 5.5×10^{-6} M	[14]
7	Microfluidic MIPs + Gibbs Reagent	Lab Sample	0.25-10 ppm	[27]
8	Microfluidic MIPs + Electrochemical	Lab Sample	$<5 \times 10^{-6}$ M	[29]

REFERENCES

(1) Baker, M. T.; Naguib, M. *Anesthesiology* **2005**, *103*, 860.

(2) Kam, P. C. A.; Cardone, D. *Anaesthesia* **2007**, *62*, 690.

(3) Diedrich, D. A.; Brown, D. R. *J. Intensive Care Med.* **2011**, *26*, 59.

(4) Hirota, K.; Ebina, T.; Sato, T.; Ishihara, H.; Matsuki, A. *Acta Anaesthesiol. Scand.* **1999**, *43*, 842.

(5) Anaesthesia UK. Target Controlled Infusions [TCI] in aneasthetic practice. http://www.frca.co.uk/articly.aspx?articleide=101001. (accessed Sep 27, 2011).

(6) Thompson, K. A.; Goodale, D. B. *Intens. Care Med.* **2000**, *26*, S400.

(7) Plummer, G. F. *J. Chromatogr. B.* **1987**, *421*, 171.

(8) Adam, H. K.; Douglas, E. J.; Plummer, G. F.; Cosgrove, M. B. *J. Chromatogr.* **1981**, *223*, 232.

(9) Lowe, E.R.; Banks, C.E.; Compton, R.G. *Ana.l Bional. Chem.* **2005**, *383*, 523.

(9) Uebel, R. A.; Wium, C. A.; Hawtrey, A. O.; Coetzee, J. *J. Chromatogr. B.* **1990**, *526*, 293.

(10) Pissinis, D. E.; Marioli, J. M. *J. Liq. Chromatogr. Relat. Technol.* **2007**, *30*, 1787.

(11) Yeganeh, M. H.; Ramzan, I. *J. Chromatogr. B.* **1997**, *691*, 478.

(12) Gibbs, H. D. *J. Biol. Chem.* **1927**, *72*, 649.

(13) Wang, J.; Jiang, M.; Lu, F. *J. Electroanal. Chem.* **1998**, *444*, 127.

(14) Langmaier, J.; Garay, F.; Kivlehan, F.; Chaum, E.; Lindner, E. *Anal. Chim. Acta* **2011**, *704*, 63.

(15) Petcu, M.; Schaare, P. N.; Cook, C. J. *Anal. Chim. Acta* **2004**, *504*, 73.

(16) Thiagarajan, S.; Cheng, C.-Y.; Chen, S.-M.; Tsai, T.-H. *J. Solid State Electrochem.* **2011**, *15*, 781.

(17) Costentin, C.; Louault, C.; Robert, M.; Savéant, J.-M. *PNAS* **2009**, *106*, 18143.

(18) Lezna, R.O.; de Tacconi, N.R.; Centeno, S.A.; Arvia, A.J. *Langmuir* **1991**, 7, 1241.

(19) Shannon, C.; Frank, D.G.; Hubbard, A.T. *Annu. Rev. Phys. Chem.* **1991**, *42*, 393.

(20) Chaum, E.; Lindner, E.; Curley, K. C.; Guo, J. The University of Tennessee Research Foundation, USA; The University of Memphis Research Foundation; United States Dept. of the Army . 2010, p 67pp.

(21) Laurila, T.; Sorvajarvi, T.; Saarela, J.; Toivonen, J.; Wheeler, D. W.; Ciaffoni, L.; Ritchie, G. A. D.; Kaminski, C. F. *Anal. Chem.* **2011**, *83*, 3963.

(22) Hornuss, C.; Praun, S.; Villinger, J.; Dornauer, A.; Moehnle, P.; Dolch, M.; Weninger, E.; Chouker, A.; Feil, C.; Briegel, J.; Thiel, M.; Schelling, G. *Anesthesiology* **2007**, *106*, 665.

(23) Takita, A.; Masui, K.; Kazama, T. *Anesthesiology* **2007**, *106*, 659.

(24) Miekisch, W.; Fuchs, P.; Kamysek, S.; Neumann, C.; Schubert, J. K. *Clin. Chim. Acta* **2008**, *395*, 32.

(25) Gong, Y.; Li, E.; Xu, G.; Wang, H.; Wang, C.; Li, P.; He, Y. *J. Int. Med. Res.* **2009**, *37*, 1465.

(26) Petcu, M.; Cooney, J.; Cook, C.; Lauren, D.; Schaare, P.; Holland, P. *Anal. Chim. Acta* **2001**, *435*, 49.

(27) Hong, C.-C.; Chang, P.-H.; Lin, C.-C.; Hong, C.-L. *Biosens. Bioelectron.* **2010**, *25*, 2058.

(28) Yeh, W.-M.; Ho, K.-C. *Anal. Chim. Acta* **2005**, *542*, 76.

(29) Fowler, S. A. The development of sensors for the detection of clinically relevant substances using molecular imprinting Ph.D. Thesis, Cranfield University, 2009.

CHAPTER 2 : ELECTROCHEMICAL TECHNIQUES

THREE ELECTRODE SETUP

For voltammetric experiments, a three electrode setup is used. This consists of a working electrode (WE), reference electrode (RE), and a counter electrode (CE). The working electrode is made from inert materials that are good electron conductors (*e.g.* gold or platinum) or semiconductors (*e.g.* p-GaP). It is at the working electrode where the electrochemical reaction of interest occurs. The reference electrode is necessary in order to provide a stable and accurate potential to be used as a reference voltage. A typical three electrode setup is portrayed in Fig. 2.1. The electrochemical cell can be controlled by an external potentiostat.

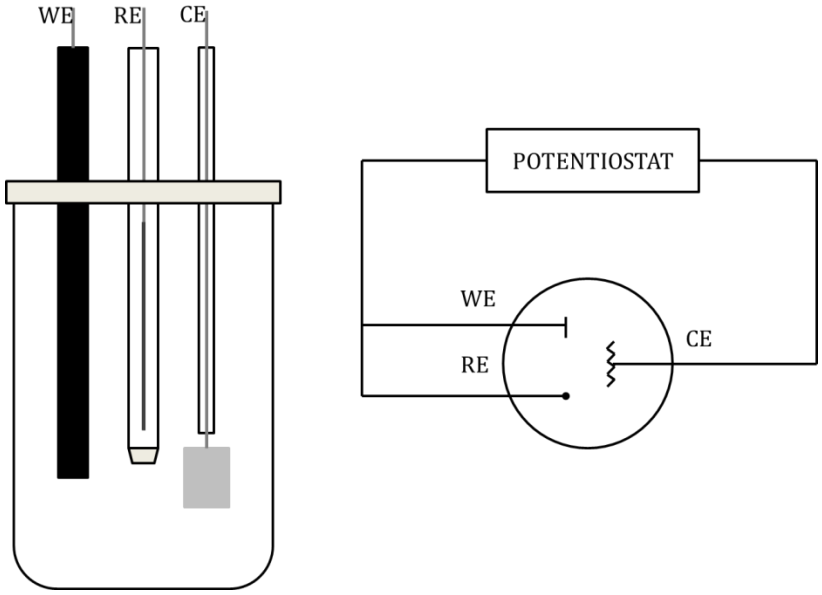

Fig. 2.1 Typical three electrode electrochemical cell.

When only small currents are being measured such as in microelectrode studies, a working electrode and reference electrode are sufficient. However, for the use of macroelectrodes and larger currents, the system becomes more complicated. Assuming a working and reference electrode with a finite current flowing between them,

$$E = (\varphi_m - \varphi_s) + iR + (\varphi_s - \varphi_{ref}) \quad \text{Eq. 2.1}$$

where the potential is described as the sum of three terms and φ refers to the Galvani potential. The first term, (φ_m-φ_s) refers to the potential difference between the electrode and the solution, which describes the electrolysis at the working electrode. The second term, *iR*, is often referred to as the Ohmic drop and is due to the resistance of the solution between the two electrodes. The third term, (φ_s-φ_{ref}) is the potential drop at the reference electrode and is determined by the chemical composition of the reference electrode. With small currents, *iR* is negligible and (φ_s-φ_{ref}) is constant. However, when large currents are used—characteristic of large electrodes, (φ_s-φ_{ref}) does not remain constant. To remedy this problem, a counter electrode is used to avoid large destabilising currents between the working and reference electrodes.[1,2]

CYCLIC VOLTAMMETRY

Cyclic voltammetry (CV) is a powerful electrochemical technique and the most widely used. In this technique, the current is measured as a function of the applied potential. As a potential sweep technique, the potential is swept from an initial potential, E_1, to a vertex potential, E_2. This is done at a constant rate, with respect to time, and is referred to as the scan rate, ν. Upon reaching E_2, the scan is reversed, at the same rate, and the potential is swept back to E_1. This creates a triangular waveform, as described in Fig. 2.2. In reality, many modern instruments are digital, and thus scan in a staircase fashion of minute increments. Provided that the increments in potential are minute, stepwise scanning is equivalent to a linear sweep, but larger increments will result in a shift in peak potentials.[3]

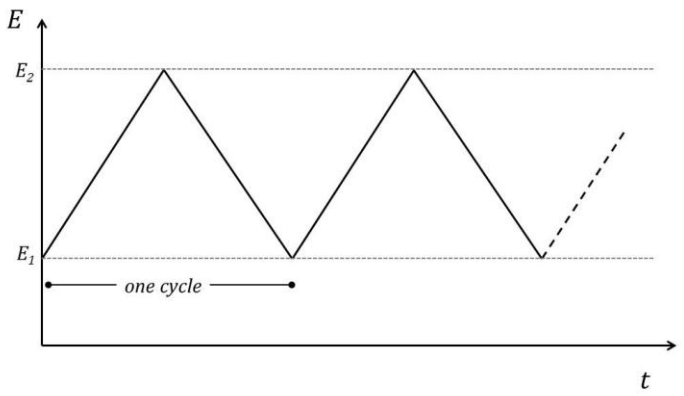

Fig. 2.2 Triangular waveform of a cyclic voltammogram. Potential is swept from E_1 to E_2 back to E_1 for one cycle. This can be repeated n times.

Given the redox active species, R which oxidises to O,

$$R_{(aq)} \rightleftharpoons O_{(aq)} + e^-_{(m)}$$

as the potential at the working electrode reaches the oxidation potential, R will oxidise to O and an exponential increase in current will occur. Replenishment of R at the electrode from the bulk solution is limited and so as R becomes depleted at the electrode surface, the current increases less exponentially and eventually a maximum peak current, i_p, is reached. As the scan is reversed and more reducing potentials are achieved, the opposite occurs as O is reduced to R. This results in a cyclic voltammogram as depicted in Fig. 2.3.

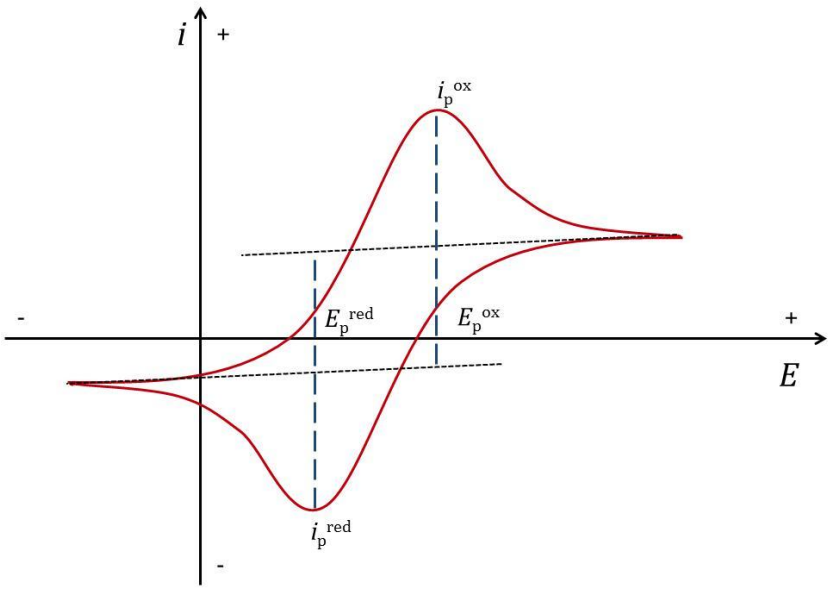

Fig. 2.3 A typical cyclic voltammogram for a reversible reaction showing oxidation and reduction peaks.

In a reversible (Nernstian or fast electron-transfer kinetics) electron transfer process, E_p^{red} and E_p^{ox} are separated by $\frac{59}{n}$ mV at 298K where n is the number of electrons transferred per mole of reagent. The peak currents, i_p^{ox} and i_p^{red}, can be described by the Randles-Sevčik equation (Eq. 2.2).

$$i_p = 0.4463\, nFAC\left(\frac{nF\nu D}{RT}\right)^{\frac{1}{2}} \qquad \text{Eq. 2.2}$$

Where n is the number of electrons transferred in the redox process, F is the Faraday Constant in C mol^{-1}, A is the area of the electrode in cm^2, C is the concentration in mol cm^{-3}, D is the diffusion coefficient in cm^2 s^{-1}, R is the ideal gas constant, T is the temperature, and ν is the scan rate in V s^{-1}. For experiments at 298 K, the expression simplifies to

$$i_p = 2.69 \times 10^5\, n^{\frac{3}{2}} AD^{\frac{1}{2}} C\nu^{\frac{1}{2}} \qquad \text{Eq. 2.3}$$

Therefore, the magnitude of the peak current is dependent on scan rate and is directly proportional to the concentration. Thus, CV can be used as a quantitative analytical technique.[1,2,4]

The kinetics of CV are governed by electron transfer and mass transfer, as outlined in Fig. 2.4. The electron transfer step occurs at the electrode surface and is governed by the energies of the electrode (Fermi Level) and the redox species in solution. The mass transfer step is determined by the diffusion of the redox species from the bulk solution.[1]

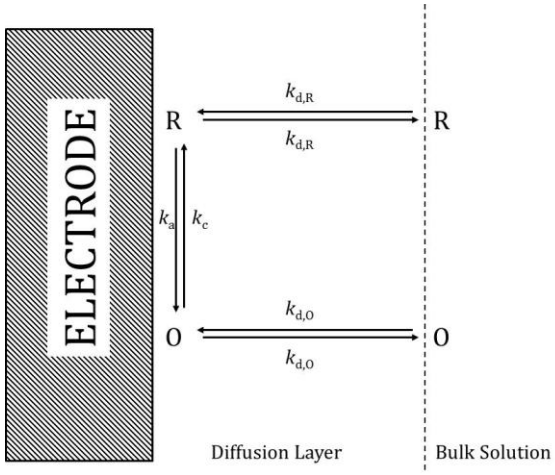

Fig. 2.4 Kinetic processes governing electrochemical experiments. The terms k_a and k_c are the rate constants for the electron transfer step and the terms $k_{d,R}$ and $k_{d,O}$ are the rate constants for diffusion between the electrode surface and the bulk solution (mass transfer).

As well as a concentration gradient, an electrical field gradient is established as a result of a difference in charge between the electrode and the solution. The layering and gradient are described by the electrolyte double layer model, which is depicted in Fig. 2.5. As a result of charge separation, the double layer acts as a capacitor and is responsible for the capacitive current, which is recorded along with the Faradaic current.

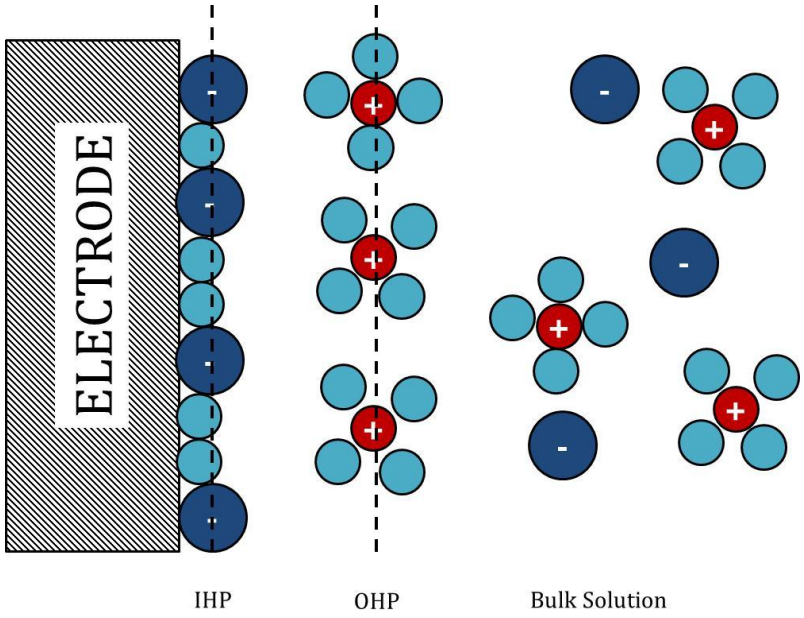

Fig. 2.5 The electrolyte double layer. IHP is the inner Helmholtz plane, and OHP is the outer Helmholtz place. The orientation of the charges is dependent on the charging of the electrode.

Because the Faradaic current is imposed upon the capacitive current, it is necessary to correct for this when measuring i_p^{ox} and i_p^{red}. This can be done simply by subtracting out the current measured in a background scan.[4] The capacitive current can also be reduced by decreasing the electrode surface area or by employing pulse techniques.

CHRONOAMPEROMETRY

Chronoamperometry (CA) is the simplest of all step techniques, and in fact, one of the simplest electrochemical techniques. In CA, the potential is initially set below the potential at which the intended reaction occurs. After a given time, the potential is then instantaneously stepped up to the potential at which the reaction is kinetically driven (mass-transfer control). Initially, a large current is recorded, which decays over time as controlled by diffusion to the electrode surface, as depicted in Fig. 2.6. Theoretically, this current spike should be infinite, but due to instrumental limitations, this is not seen.

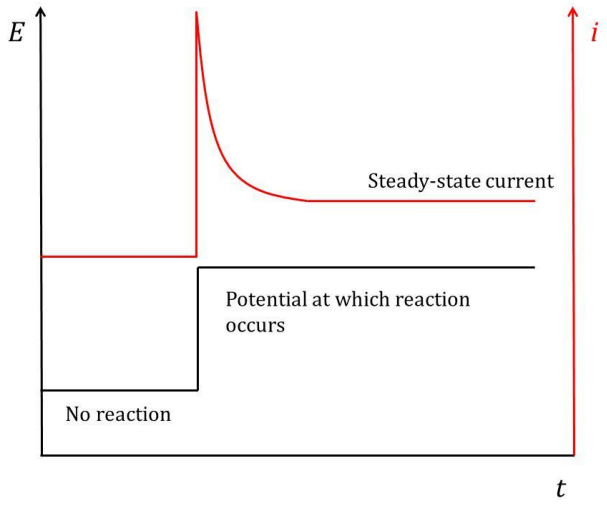

Fig. 2.6 CA potential waveform (black) and current response (red) with respect to time. Eventually a steady state current is achieved.

DIFFERENTIAL PULSE VOLTAMMETRY

In differential pulse voltammetry (DPV), the potential waveform used is a combination of pulses imposed on a staircase, as shown in Fig. 2.7. The current is measured before the

start of the pulse and before the pulse is finished. The difference in current is then plotted with respect to potential.

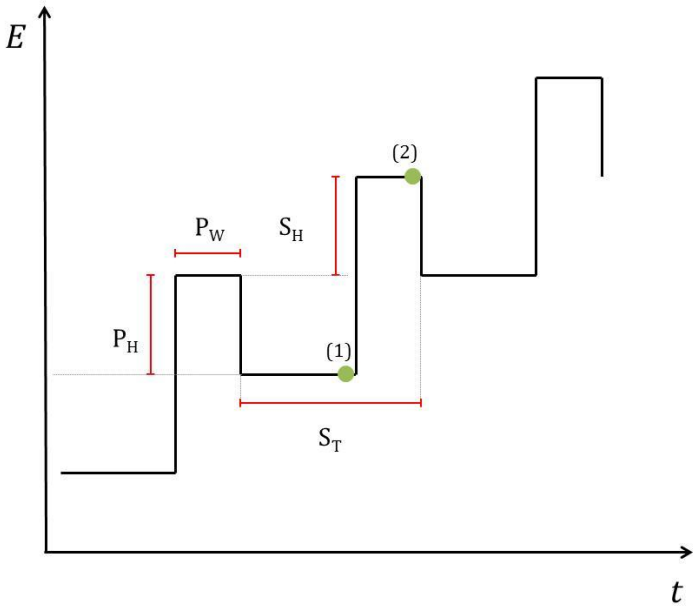

Fig. 2.7 DPV waveform, with parameters labelled as used in experiments reported here. P_H is pulse height, P_W is pulse width, S_T is step time, and S_H is step height. The green points indicate where the current is measured with respect to each step, where $\Delta I = I(2) - I(1)$.

The peak current is given by the expression

$$i_p = \frac{nFAD^{\frac{1}{2}}C}{(\pi t_m)^{\frac{1}{2}}}\left(\frac{1-\sigma}{1+\sigma}\right) \qquad \text{Eq. 2.4}$$

where

$$\sigma = e^{\left(\frac{nF}{RT}\frac{\Delta E}{2}\right)} \qquad \text{Eq. 2.5}$$

and t_m is the pulse duration and ΔE is the pulse amplitude.[1,4]

The advantage to using DPV is that it eliminates the capacitive current, and only Faradaic current is recorded. Additionally, DPV is capable of achieving detection limits of the order of 10^{-8} M.

REFERENCES

(1) Brett, C. M. A.; Brett, A. M. O. *Electroanalysis*; Oxford University Press: Oxford, **1998**.

(2) Fisher, A. C. *Electrode Dynamics*; Oxford University Press: Oxford, **1996**.

(3) Barnes, A.S; Streeter, I.; Compton, R.G. *J. Electroanal. Chem.* **2008**, *623* 129.

(4) Bard, A. J.; Faulkner, L. R. *Electrochemical Methods: Fundamentals and Applications*; John Wiley & Sons, Inc.: New York, **2001**.

CHAPTER 3 : FACILITATED DETECTION AT THE LIQUID-LIQUID INTERFACE

INTRODUCTION

Electrochemistry at the interface between two immiscible solutions (ITIES) and its applications have been extensively reviewed and discussed.[1-3] The information herein is to provide background knowledge for understanding electrochemistry at the ITIES and micro ITIES.

When two immiscible solutions contain electrolytes, a Galvani potential difference at the interface between them can form as a result of the differential transfer of the ions present.[4] This potential difference means that the interface can be controlled by an external potential, and, thus the interface can be used to study electron transfer reactions (like at a solid electrode) as well as ion transfer across the interface.[3,4] It is in the study of ion transfer that electrochemistry at the ITIES proves most useful and this will be discussed here.

For ion transfer between water (w) and oil or organic (o) phases, the Gibbs energy of transfer ($\Delta G^{0,w\rightarrow o}_{transfer,i}$) must be given to the ion in order for it to transfer from one phase to the other. This is achieved by the application of a potential to the interface, polarising it so the Galvani potential difference is defined as

$$\Delta_o^w \phi = \phi^w - \phi^o \qquad \text{Eq. 3.1}$$

At equilibrium, the Nernst equation for ion transfer reactions is then given as

$$\Delta_o^w \phi = \Delta_o^w \phi_i^0 + \frac{RT}{z_i F} \ln\left(\frac{a_i^o}{a_i^w}\right) \qquad \text{Eq. 3.2}$$

where a_i is the activity of ion i, and z_i is the charge. The Gibbs energy of transfer is related to the standard potential of transfer $\Delta_o^w \phi_i^0$ in its definition

$$\phi_i^0 = \frac{\Delta G_{transfer,i}^{0,w\to o}}{z_i F} = \frac{\mu_i^o(o) - \mu_i^o(w)}{z_i F} \qquad \text{Eq. 3.3}$$

The control of the potential at the interface can be achieved by a four-electrode system. A pair of counter and a pair of reference electrodes are used, with one each phase of the system.[1] Typically, the reference electrodes are connected to the system via Luggin capillaries, with tips proximal to the interface, as described in Fig. 3.1 below.

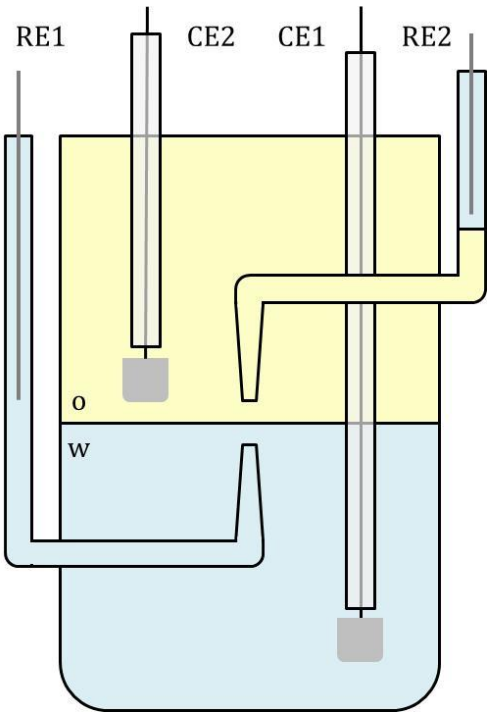

Fig. 3.1 Scheme for four-electrode controlled electrochemical cell for polarisation of the ITIES. o and w denote oil and water phases; RE reference electrode; CE counter electrode.

This cell (Fig. 3.1) has three major components along with the reference electrodes and can be described by

$$\text{RE|RX(w')|SY(o)||RX(w)|RE} \qquad \text{Eq. 3.4}$$

Phase boundaries exist between the aqueous reference [RX(w')] and the oil (SY), and between the oil and the aqueous phase (RX). A typical setup for studying the transfer of the tetraphenylborate ion (TPB^-) would be as follows

$$\text{Ag|AgCl|LiCl}_{(aq)}\text{|TBATPB}_{(o)}\text{||TBACl}_{(aq)}\text{|AgCl|Ag} \qquad \text{Eq. 3.5}$$

Just as in the case of solid electrodes, when voltammetric techniques are applied, the peak currents, relating to ion transfer, are governed by the Randles-Sevčik equation. Additional terms are incorporated, however, to describe the nature of ion transfer and not electron transfer. And like solid electrodes, minimising the area of the interface eliminates capacitive current. For a micropipette system, the current is governed by

$$i_{pip} = 3.35\pi nFaDC \qquad \text{Eq. 3.6}$$

where all terms retain their meanings from the Randles-Sevčik equation except D is the diffusion coefficient of the species in the outer solution.[5] Additionally, with micropipettes, because the current flowing between the electrodes is so small, the need for counter electrodes is eliminated.

Kinetically, ion transfer can be described in three phases. First there is mass transfer to the interface, which is predominantly by diffusion. Second is the ion transfer reaction as the ion crosses the interface. Finally, there is the mass transfer in the other phase away from the interface. The dynamics of transfer can be modified by the use of ligands which facilitate ion transfer across the interface.[3]

Facilitated transfer of ions across the ITIES involves the use of a neutral ligand to aid ion transfer across the interface. There are many ways possible in which this could be achieved and depends on the relative concentrations and where the ligand is located. Facilitated ion transfer reactions, however, can be described by one of four mechanisms. These mechanisms depend primarily on where complexation occurs in reference to the interface—either at the interface, or within one of the two phases.[3]

Mechanisms in which the complexation occurs in one of the two phases are *aqueous complex transfer* (ACT) and *transfer followed by organic phase complexation* (TOC). In the former case, the ion complexes with the ligand in the aqueous phase and is then transferred to the organic phase as a complex. In the latter, the ligand is located in the organic phase and so the ion transfers from the aqueous phase to the organic phase and then complexes with the ligand.[3,6]

The mechanisms in which complexation occurs at the interface are *transfer by interfacial complexation* (TIC) and *transfer by interfacial dissociation* (TID). The TIC mechanism describes a process where the ion complexes with the ligand at the interface and is then transported to the other phase as a complex. The TID mechanism is the opposite, where the ion is transported to the interface as a complex and then dissociates at the interface.[3,6]

Ligands used for assisted transfer can range from macromolecules to proteins.[3,5,7,8] Popular macromolecular ligands include crown ethers, such as dibenzo-18-crown-6, as well as cyclodextrins.[8] Cyclodextrins are an interesting class of ligands, particularly because of the variety available. They are macromolecules containing six, seven, or eight glucose molecules and are classed as α-, β-, and γ-cyclodextrins, respectively.

Structurally, β-cyclodextrins can described as a toroid structure with a highly hydrophobic inner core, as depicted in Fig. 3.2.[9]

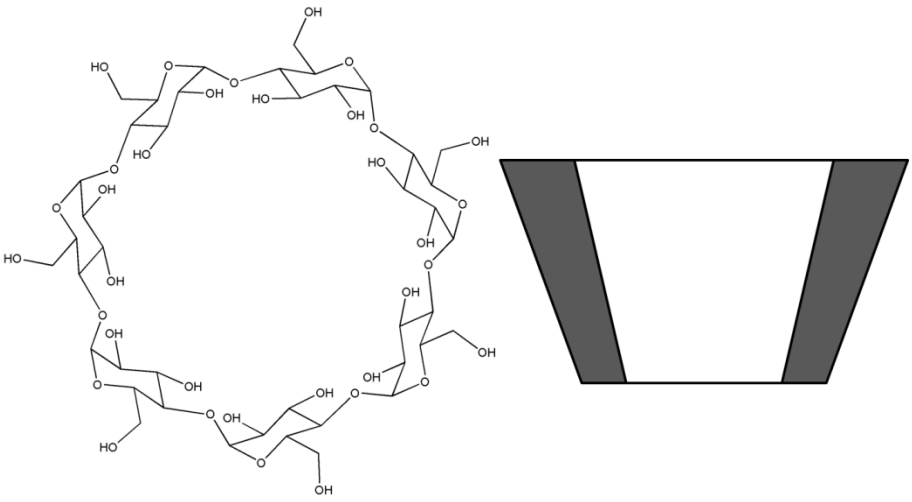

Fig. 3.2 Chemical and physical structures of β-cyclodextrins.

The class of β-cyclodextrins are of particular interest to this work as propofol is known to complex with these sugar macromolecules, and their interaction has been well characterised.[10] Propofol forms a 1:1 complex with β-cyclodextrins in solution. The stability constant of the complex, $K_{1:1}$, has been reported as 3439 M^{-1} for a complex of propofol and 2-hydroxypropyl-β-cyclodextrin at 25 °C and pH 6.5 and it has been shown that β-cyclodextrins can increase the aqueous solubility of propofol from around 840 μM to concentrations over 260-fold greater.[11] There even exist formulations of the drug for delivery which use β-cyclodextrins to help solubilise the propofol.[12] Electrochemistry at the μITIES could, therefore be a powerful tool, capitalising on this drug-ligand interaction for the detection of propofol.

However, ligand facilitated transfer at the ITIES of propofol is not as straightforward as one might think. In the literature, ITIES has only been used to study ionic analytes. The challenge with propofol is that propofol is not easily ionisable, and, therefore must be treated as a neutral molecule. The question that then arises is, can the transfer of a non-ionic species at the ITIES be controlled and detected electrochemically? The hypothesis

used to try to answer this question relies on the reversal of the conventional ion-ligand facilitated transfer system. Rather than using a neutral ligand to facilitate the transfer of a charged ion, it is proposed that a charged ligand could be used to facilitate the transfer of a non-charged molecule. The system used to test this hypothesis uses propofol as the neutral molecule and the phosphated β-cyclodextrin sodium salt $C_{42}H_{70}O_{47}P_4Na_4$ (NaPβCD) as the charged ligand.

METHODS

To study the transfer of propofol at the μITIES, an electrochemical cell consisting of a glass micropipette and a U-tube was used, as described in Fig. 3.3. Micropipettes were fashioned from borosilicate glass capillaries (Harvard Apparatus, Ltd., UK) with an outer diameter of 1.5 mm and an inner diameter of 1.17 mm by means of a Model P-97 Flaming/Brown micropipette puller (Sutter Instrument Co., USA). The parameters used were H: 480, V: 25, and T: 250.

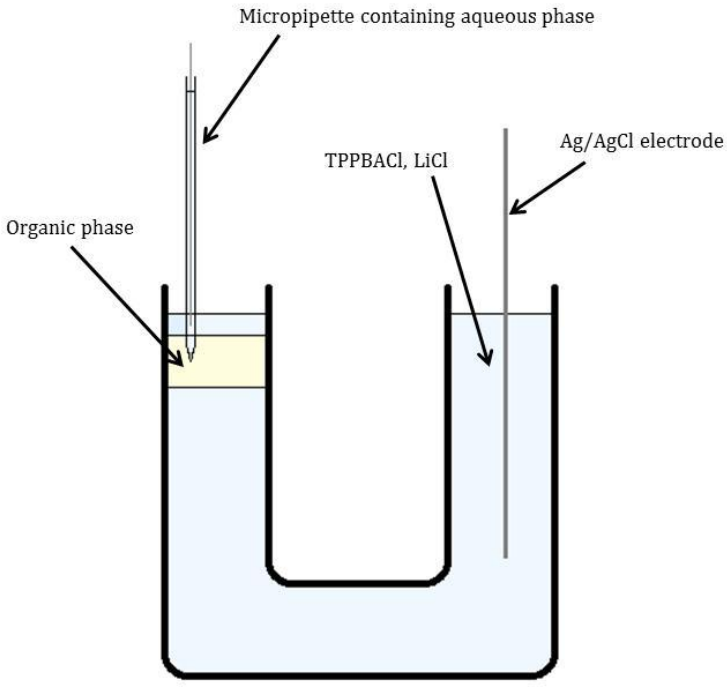

Fig. 3.3 U-tube setup for studying propofol transfer at the μITIES. Propofol was added to the organic phase and cyclodextrins were added to the aqueous phase filling solution in the micropipette.

Unless otherwise stated, all reagents used were provided by Sigma-Aldrich, UK. The supporting aqueous phase was a 10 mM solution of tetrabutylammonium chloride (TBACl) ≥97%. The supporting electrolyte was also layered on top of the organic layer to prevent any evaporation. The organic phase contained the electrolyte tetrabutylammonium tetraphenylborate (TBATPB) ≥99% at a concentration of 10 mM and was consistently measured out to 300 μL. The micropipette was filled by syringe with 10 mM $LiCl_{(aq)}$ solution. This is the same electrochemical cell as describe by Eq. 3.5. When used, propofol was dissolved in the organic phase and the β-cyclodextrin in the aqueous phase of the micropipette. Cycloheptaamylose was purchased from Sigma-Aldrich, UK and the phosphated β-cyclodextrin NaPβCD was purchased from CycloLab, Hungary. These were both the simplest charged and uncharged β-cyclodextrins available. The reference electrodes were prepared by immersing two Ag wires in saturated KCl solution and applying potentials of 2.0 V and -2.0 V for 15 minutes each.

For experiments with cycloheptaamylose, the cell was controlled by an AUTOLAB PGSTAT12 potentiostat (Windsor Scientific, UK). For experiments with NaPβCD, the cell was controlled by a VMP Multichannel Potentiostat (Perkin Elmer Instruments). CV and DPV were used to study the system. CVs were conducted at varying scan rates, and the parameters for DPV experiments are as follows: P_H=2.5 mV, P_W=100 ms, S_H=5 mV, S_T=500 ms.

UV spectroscopy was used to investigate whether or not propofol is able to cross the ITIES without the application of an external potential. An aqueous layer of 10 mM LiCl and 10 mM of NaPβCD was stratified on top of an organic layer of 10 mM TBATPB and 50 mM propofol. Samples of the aqueous component were analysed by a UV-Vis spectrophotometer (Unicam UV2) before stratification and after 30 minutes.

RESULTS & DISCUSSION

Cycloheptaamylose as a ligand for propofol transfer

Cyclic voltammograms of the background cell (Eq. 3.5) show a potential window from 0 to 0.5 V, as seen in Fig. 3.4. Upon addition of 50 mM of propofol to the system, there were no significant differences apart from the intensity of the measured currents. Given the high lipophilicity of propofol, this is likely due to an increase in resistance at the interface. The lack of any current peaks indicates that there is no transfer across the interface within the given potential window.

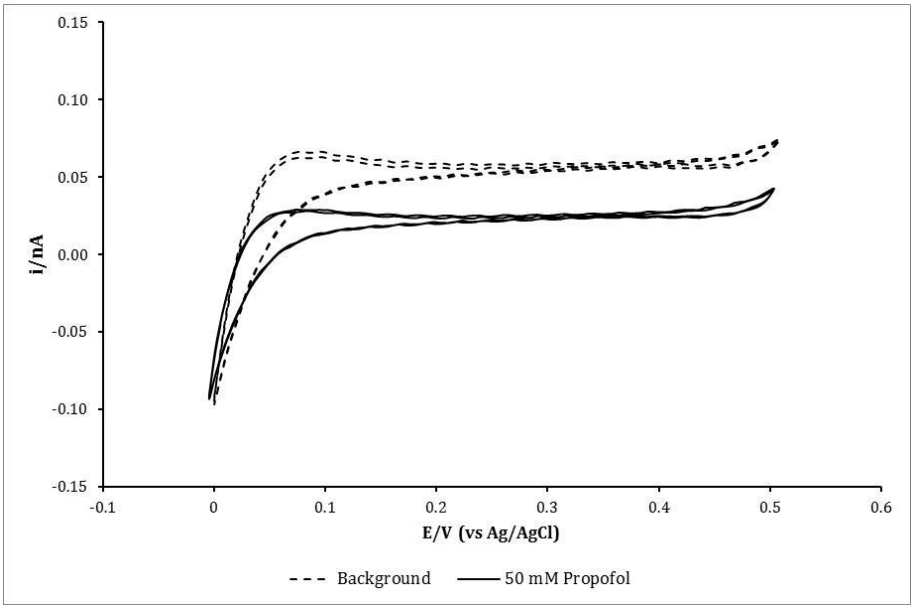

Fig. 3.4 CV taken at 100 mV s^{-1} of the background system (dashed) and 50 mM of propofol in the organic phase (solid).

Upon the addition of 10 mM of the uncharged β-cyclodextrin cycloheptaamylose, the CV profile changed dramatically, suggesting some sort of transfer process, as shown in Fig. 3.5. However these results were not consistently reproducible. Rather than being indicative of transfer, the increase in current around 0.4 V could be indicative of complexation at the interface, but not necessarily transfer.

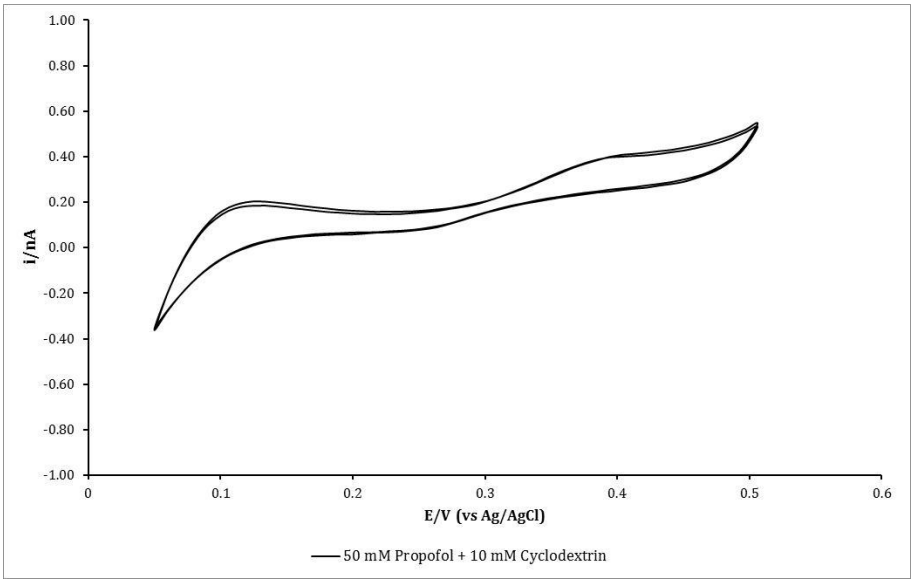

Fig. 3.5 CV taken at 100 mV s^{-1} of 50 mM propofol opposed by 10 mM cycloheptaamylose at the μITIES.

Charged cyclodextrins for facilitated transfer

With propofol in the organic phase, it was able to be detected by DPV as a change in the current corresponding to the transfer of NaPβCD. This is shown in Fig. 3.6. Fig. 3.7 gives the peak currents as a function of propofol, and from it, it can be argued that there is a positive correlation between current and propofol concentration in the organic phase. This trend only exists up to equimolar concentrations, suggesting that the system is controlled by propofol as it facilitates the transfer of NaPβCD. Clearly, more repetitions are required and a broader range of concentrations should be used before any conclusive remarks can be made.

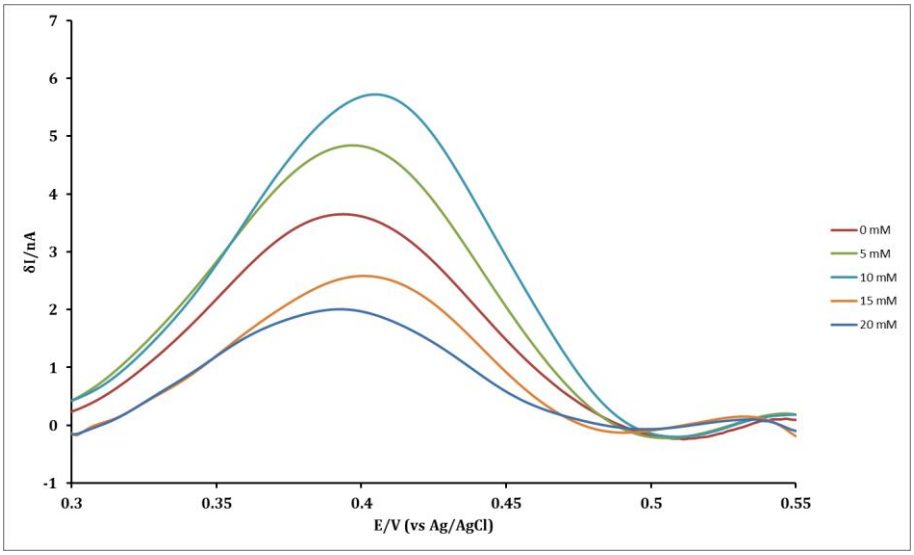

Fig. 3.6 Baseline corrected DPVs showing the effect of propofol on the transfer of 10 mM NaPβCD.

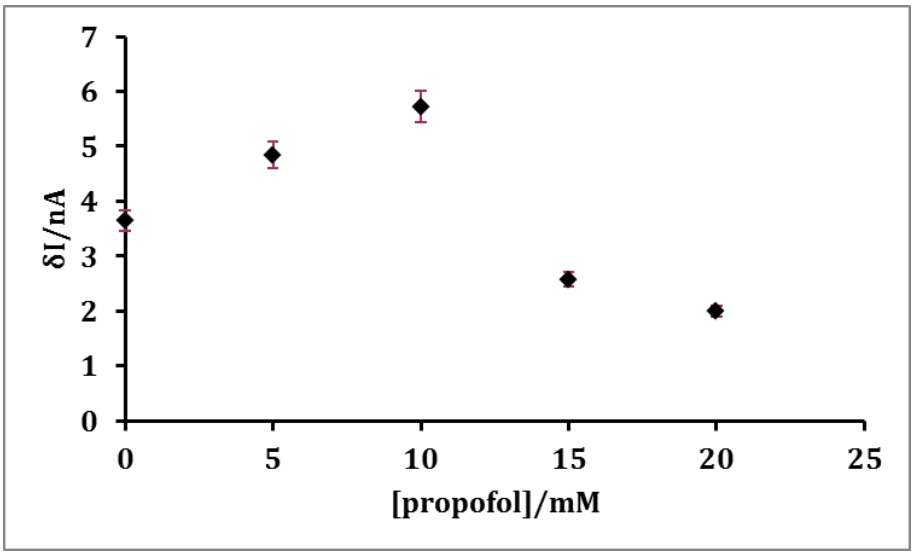

Fig. 3.7 Absolute difference in *δI* plotted against the concentration of propofol. Error bars ±5%.

UV spectroscopy

In an aqueous solution of 10 mM β-cyclodextrin, propofol should be soluble up to a concentration of 5 mM, according to calculations based on data from Trapani *et al.*[11] This is nearly six times the normal solubility of propofol in an aqueous solution. Given the large difference in propofol concentration across the boundary (i.e., 5-20 mM versus 0 mM) and the increased capacity of the cyclodextrins containing aqueous solution to dissolve propofol, it is possible that propofol could diffuse between the two phases. If

propofol can diffuse from the organic to the aqueous phase without an external potential, then it could be suggested that the system is governed by the ACT mechanism, as shown in Fig. 3.8A. UV spectroscopy did not identify a change in absorbance for propofol at 276 nm before and after 30 minutes of exposure of the aqueous layer to the propofol containing organic layer. This would confirm that complexation between NaPβCD and propofol occurs at the interface. The two models are described in Fig. 3.8.

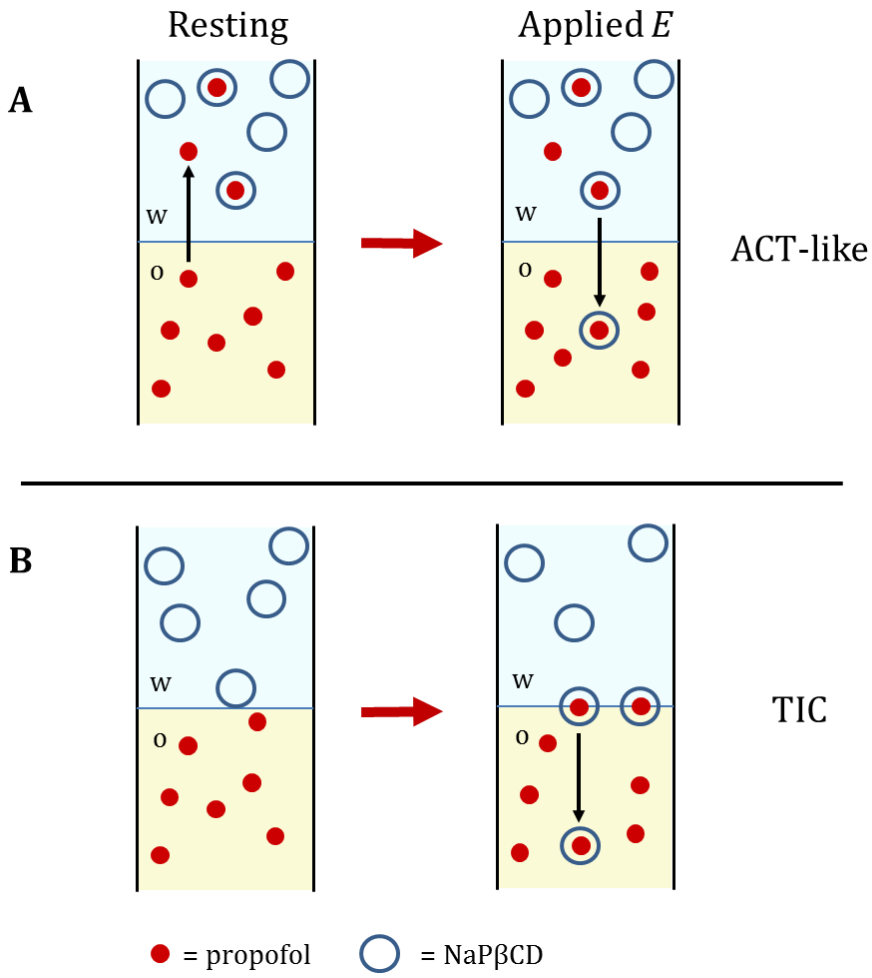

Fig. 3.8 Two models for transfer at the ITIES involving propofol and NaPβCD. In model A, propofol is able to diffuse from a high concentration in the organic (yellow) phase across the ITIES to the aqueous phase (blue) where it complexes with the cyclodextrins. When a potential is applied, the complex crosses the interface. Its increased mass (compared to the cyclodextrins on its own), results in a decreased current. In model B, propofol cannot enter into the aqueous phase. Upon the application of a potential, propofol complexes with NaPβCD at the interface and the complex is transferred.

CONCLUSIONS

Although further investigation is required, it was demonstrated that propofol affects the transfer of NaPβCD at the μITIES. It may be that a charged ligand can be used for the detection of a non-charged analyte at the μITIES. The mechanism by which propofol and NaPβCD transfer and complex is most likely the TIC mechanism, but more thorough analysis is required. Experiments studying the ratio of diffusion coefficients of propofol and the complex in the organic phase as well as a better understanding of the solubility of the complex in both organic and aqueous phases are required to conclusively determine by which mechanism facilitated transfer is occurring. In doing so, the geometries of the diffusion fields will need to be taken into account.[6] Additionally, a greater range of concentrations of propofol should be used when the cyclodextrin is kept in excess. The reverse process (the transfer of the ligand from the complex to the aqueous phase) would also shed light on the process.

REFERENCES

(1) Samec, Z. *Pure Appl. Chem.* **2004**, *76*, 2147.

(2) Samec, Z.; Samcova, E.; Girault, H. H. *Talanta* **2004**, *63*, 21.

(3) Reymond, F.; Fermin, D.; Lee, H. J.; Girault, H. H. *Electrochim. Acta* **2000**, *45*, 2647.

(4) Bard, A. J.; Faulkner, L. R. *Electrochemical Methods: Fundamentals and Applications*; John Wiley & Sons, Inc.: New York, 2001.

(5) Beattie, P. D.; Delay, A.; Girault, H. H. *J. Electroanal. Chem.* **1995**, *380*, 167.

(6) Shao, Y.; Osborne, M. D.; Girault, H. H. *J. Electroanal. Chem.* **1991**, *318*, 101.

(7) Collins, C. J.; Lyons, C.; Strutwolf, J.; Arrigan, D. W. M. *Talanta* **2010**, *80*, 1993.

(8) Kataky, R.; Lopes, P. *Chem. Commun.* **2009**, 1490.

(9) Ferancova, A.; Labuda, J. *Fresen. J. Anal. Chem.* **2001**, *370*, 1.

(10) Trapani, G.; Latrofa, A.; Franco, M.; Lopedota, A.; Sanna, E.; Liso, G. *J. Pharm. Sci.* **1998**, *87*, 514.

(11) Trapani, G.; Lopedota, A.; Franco, M.; Latrofa, A.; Liso, G. *Int. J. Pharm.* **1996**, *139*, 215.

(12) Baker, M. T.; Naguib, M. *Anesthesiology* **2005**, *103*, 860.

CHAPTER 4 : MODIFIED CARBON ELECTRODES

INTRODUCTION

Chemically modified electrodes (CMEs) offer an approach to electrode systems leading to considerable utility and functionality.[1] Modifying an electrode surface can offer advantages such as an increased surface area, a platform to investigate surface coatings, new chemical functionality—including selectivity and catalytic functionalities—or to add a biological activity.[2] Modifications can include physically adsorbed surface coatings,[3] monolayers,[4] covalently bound modifiers,[5] and electrochemical pre-treatment and pre-conditioning.[6,7] This introduction will look at the use of carbon nanotubes (CNTs), β-cyclodextrins, electrochemical pre-treatment and pre-conditioning, and redox catalysts as electrode modifiers as a context for CME for propofol detection.

Carbon nanotubes

Since their re-discovery in 1991,[8] carbon nanotubes have garnered much interest amongst the scientific community and have been put to use in a variety of applications. Structurally, CNTs can be described as rolled sheets of graphene, and come in two varieties—single-wall carbon nanotubes (SWNT) and multiwall carbon nanotubes (MWNT). Both types of CNTs have two different reactive sites—edge-plane sites and basal-plane sites. Edge-plane sites are found at tube ends and are akin to the edge of a sheet of paper, whereas basal-plane sites can be likened to the surface of a sheet of paper. It has been shown by Banks *et al*[9]. that it is the edge-plane site (*i.e.*, the ends of the CNT) or similar defects on the CNT surface that offer an electrocatalytic advantage. This electrocatalytic effect is similar to that seen by using edge-plane pyrolytic graphite electrodes, but their nanostructure makes them suitable for specific applications.[9] CNTs

have found popular use in electrochemical applications, particularly in sensor and biosensor development.[10]

Electrodes modified by CNTs have been used in various sensing applications, such as the detection and discrimination of neurotransmitters. Glassy carbon electrodes (GCE) modified with MWNTs were shown to have an electrocatalytic effect on the oxidation of dopamine and serotonin, leading to an increased oxidation peak and decreased oxidation overpotential.[11] Investigations into the oxidation of NADH by Wang's group[12] showed that CNT coated electrodes were also shown to have an improved signal and decreased oxidation overpotential, but the CNT modification was also shown to decrease fouling.[12] Fouling, in the case of NADH, results when NAD^+, the oxidised form of NADH, dimerises at the electrode surface.[13] Computer simulations combined with electrochemical experiments suggest that electrode passivation is reduced due to the high surface area afforded by CNTs.[14] As this is a similar case with propofol, CNT modified electrodes might reduce surface fouling by the electrooxidation of propofol.

Apart from being used as surface modifiers, CNT paste electrodes have been reported in the literature.[15] CNT paste electrodes offer the versatility and customisation of a paste electrode in conjunction with the electronic properties of CNTs.

β-cyclodextrins

Cyclodextrins, as mentioned in Chapter 3, are cyclic macromolecular sugar molecules. The class of β-cyclodextrins consist of seven 1,4-linked D(+)-gluocopyranose molecules, with a hydrophobic core and a hydrophilic exterior. When bound to an electrode surface,

cyclodextrins can be used for electroanalytical investigations based on the formation of an inclusion complex between the hydrophobic inner core and a hydrophobic analyte. Electrochemical detection can occur in one of two ways. Either the analyte has its electroactive region exposed or the cyclodextrins has been modified with a mediator, such as ferrocene, to relay the electron transfer to the electrode surface. Electrodes can be modified by cyclodextrins in a number of ways. These include adsorption to the electrode surface, incorporation into a polymeric film, and immobilisation through covalent linkages.[16]

Thiolated β-cyclodextrins have been synthesised for their immobilisation onto gold electrodes. Self-assembled monolayers of β-cyclodextrins were shown to form well-defined layers and only allow the gold electrode to oxidise species that can enter the hydrophobic cyclodextrins cavity.[5] This effectively creates a lipophilic barrier for electron transfer discriminating against any hydrophilic electroactive species.[17]

Electrochemical pre-treatment and pre-conditioning

Pre-treatment and pre-conditioning of an electrode surface may be necessary to observe certain electrochemical behaviour. Pre-treatment involves applying certain potentials for a defined amount of time to the electrode immediately prior to an experiment. Pre-conditioning involves the repeated cycling between voltages and can be undertaken at any point in the electrode's history.[6] Electrochemical pre-treatment is known to increase the hydrophobicity of the glassy carbon electrode.[18,19] It is understood that this is the result of the introduction of carbonyl, carboxyl, and hydroxyl functionalities to the electrode surface.[7]

Pretreated electrodes for the detection of propofol have previously been discussed in Chapter 1. Work by Thiagarajan *et al.*[7] suggests that the introduction of oxygen containing functional groups to the surface of the electrode imputes an electrocatalytic effect for the electrooxidation of propofol, but no specific mechanism has been suggested.[7] It has been shown, however, that oxygen-containing surface functional groups reduce the adsorption of phenols to carbon surfaces.[20-22] GCE surfaces consist of sp^2 hybridised carbon structures, which have delocalised electrons on the surface that aid in phenolic adsorption.[23] This surface naturally contains oxygen containing function groups, as depicted in Fig. 4.1. Experiments on graphite and boron-doped graphite by Mahajan *et al.*[21] suggest that the introduction of oxygen-containing surface functional groups localises the free electrons of the carbon basal plane, thus reducing the adsorptive capacity of the surface.[21]

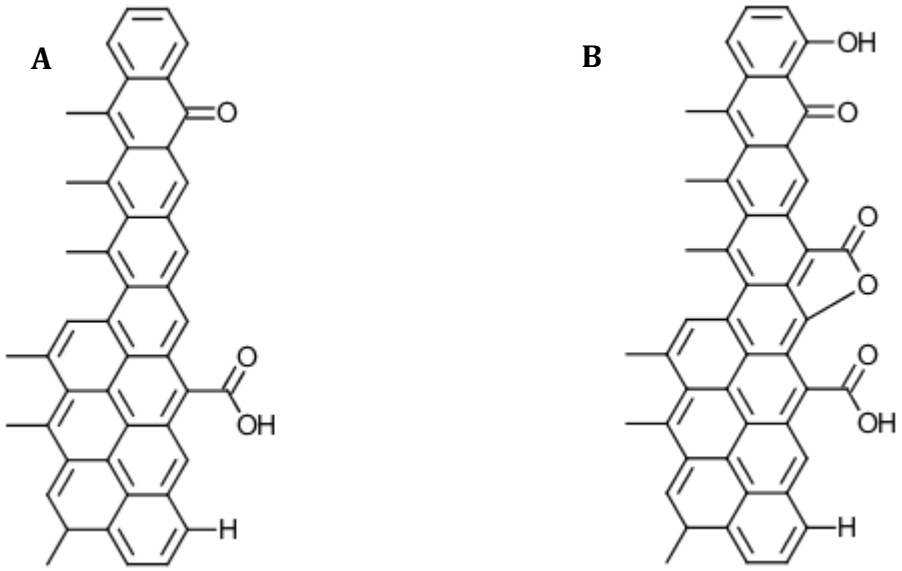

Fig. 4.1 Polished GCE surface (**A**) and GCE surface with additional oxygen containing functional groups (**B**).

Redox catalysts

Redox catalysts can also be used to modify an electrode, with the aim of catalysing the oxidation of the analyte in question. Various redox dyes have been shown to act as artificial electron donors and acceptors and such dyes can undergo electropolymerization.[24] One such dye, methylene blue (MB) (see Fig. 4.2), has been used as an electron mediator in the development of biosensors for NADH based on NADH-dehydrogenase.[25-27]

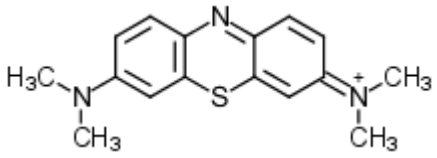

Fig. 4.2 Methylene blue

Because the electrooxidation of NADH occurs in two single-electron transfer steps, NADH can dimerise and foul the electrode.[27] After the first electron transfer step, which is widely separated in potential from the second, dimerisation with another free radical, protonation, or adsorption to the electrode surface can occur.[28] It has been shown that MB electropolymerised to gold and glassy carbon electrodes both reduces the oxidation overpotential and couples the two single-electron transfer steps into one two-electron transfer.[25,27]

Methylene blue, as a photosensitiser can produce singlet oxygen ($^1O_2$) in the presence of O_2 and light. Propofol is known to react with $^1O_2$ to form the diquinone shown in Fig. 4.3. If the diquinone is formed, then dimerisation or polymerisation of propofol will not procede. Thus, MB modified electrodes may reduce electrode fouling through $^1O_2$ production.

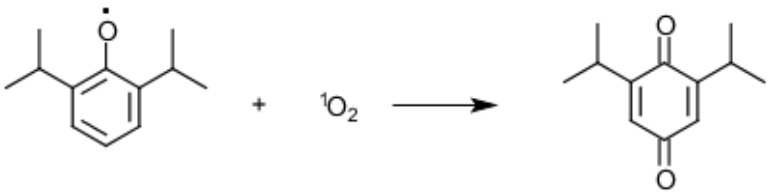

Fig. 4.3 Proposed reaction between propofol phenoxyl radical and singlet oxygen to produce a diquinone.

EXPERIMENTAL METHOD

Unless otherwise mentioned, all materials and reagents were purchase from Sigma Aldrich (UK). GCEs and modified GCEs were used as the working electrode, a platinum flag was used as the counter electrode, and a Ag/AgCl bare wire was used as the reference electrode. A VMP Multichannel Potentiostat (Perkin Elmer, UK) was used to control the electrodes. Various solutions of propofol were used and are identified where used. These include a solution of propofol prepared in phosphate buffer (PBS) and acetonitrile (ACN) (90:10 v/v) and propofol solutions in just PBS.

Glassy carbon electrodes

GCEs were polished with 0.05 μM alumina polish on a chamois surface for 2 min before being sonicated in methanol for 15 min followed by sonication in deionised water for 15 min.

CNT modified electrodes

GCEs were modified with multiwalled carbon nanotubes (MWNTs). MWNTs were dispersed in *N,N*-dimethylformamide (DMF) (2 mg/mL) solution by ultrasonic agitation for about 1 hour. GCE were modified by pipetting 6 μL of the MWNT-DMF suspension the

electrode surface of the GCE and allowed to dry. This was repeated. After modification, the electrode was rinsed in deionised water to remove any MWNTs that did not adhere.

CNT paste electrodes

CNT paste electrodes were prepared from 60% MWNTs and 40% mineral oil, by weight. The paste was then packed in the end of a poly(methyl methacrylate) tube with a diameter of 2 mm and a depth of 2 mm. Copper wire was used to connect the paste to the leads connecting to the potentiostat. This is illustrated below in Fig. 4.4. The electrode was polished on filter paper in order to pack the CNT paste and achieve a smooth surface.

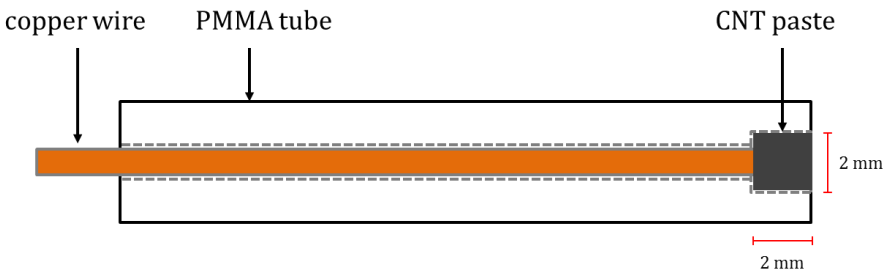

Fig. 4.4 Construction of CNT paste electrode.

β-cyclodextrin modified electrodes

To the surface of a polished GCE, 6 µL of a 2% (w/v) solution of heptakis-(2,3,6-tri-O-acetyl)-β-cyclodextrin in DCE was added. The hydrophobic cyclodextrin was used so it would not dissolve when exposed to an aqueous sample. The solvent was allowed to evaporate overnight.

Pre-anodisation

Pre-anodisation was attempted by applying CV to a polished GCE in 0.5 M H_2SO_4 between 0 and 2 V at 100 mV s^{-1}.

Methylene Blue

Solutions of 100 μM methylene blue and 400 μM propofol were prepared in 0.1 M PBS, pH 7. CV was conducted on a 50 μM solution of MB with a restricted potential window as to avoid electropolymerisation. This was repeated, but with 200 μM of propofol.

MB was then electropolymerised following the procedure reported by Karyakin *et al.*[24] A 0.02 M borate buffer was prepared from solutions of boric acid and sodium tertraborate and had a pH of 9.14. 0.1 M of KCl was used as a supporting electrolyte. A 1×10^{-3} M solution of MB was prepared in the borate buffer and a polished GCE was cycled from -0.4 to 1.2 V for 30 cycles. PolyMB coated electrodes were the used in CV and amperometric studies of propofol.

RESULTS & DISCUSSION

Glassy carbon electrode

Initially, the electrochemical properties of propofol were studied with a bare GCE. Cyclic voltammetry, displayed in Fig. 4.5 and Fig. 4.6, shows that propofol is oxidised at around 0.5 V (vs Ag/AgCl). The formation of a polypropofol product (possibly a diphenol) is evident by a second oxidation peak at 0.25 V (vs Ag/AgCl) present in cycles subsequent to the first one.

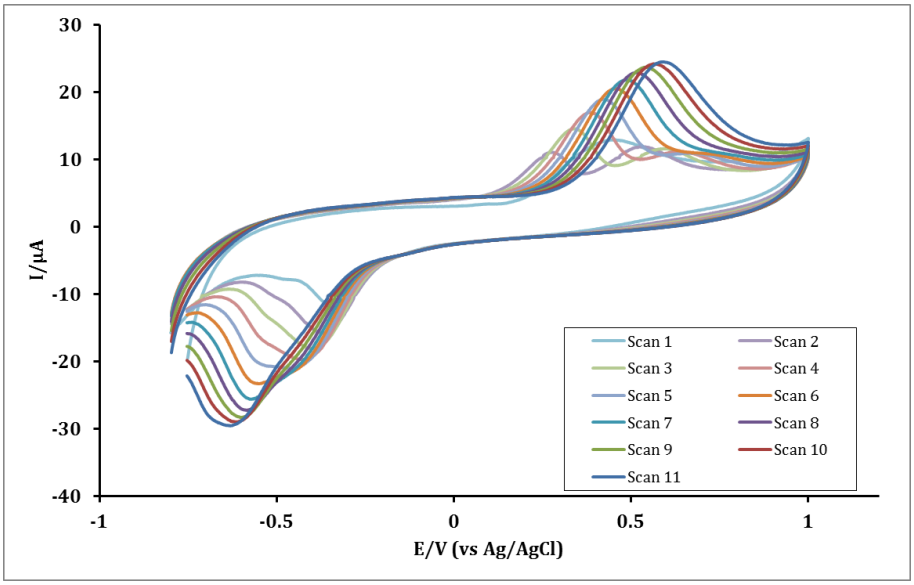

Fig. 4.5 CVs of progressive cycles of 500 μM propofol in PBS/ACN (90:10 v/v). Scan rate 100 mV s^{-1}.

The continually increasing shift between anodic and cathodic peak currents indicates that the kinetics of the electron transfer process are slowing with each successive scan.[29] This is most likely due to the formation of a film on the electrode surface which impedes electron transfer. Prior to CV experiments, the polished GCE has a shiny, reflective appearance. After use in propofol containing solutions, the electrode loses its lustre and appears darker, suggesting the deposition of a film on its surface.

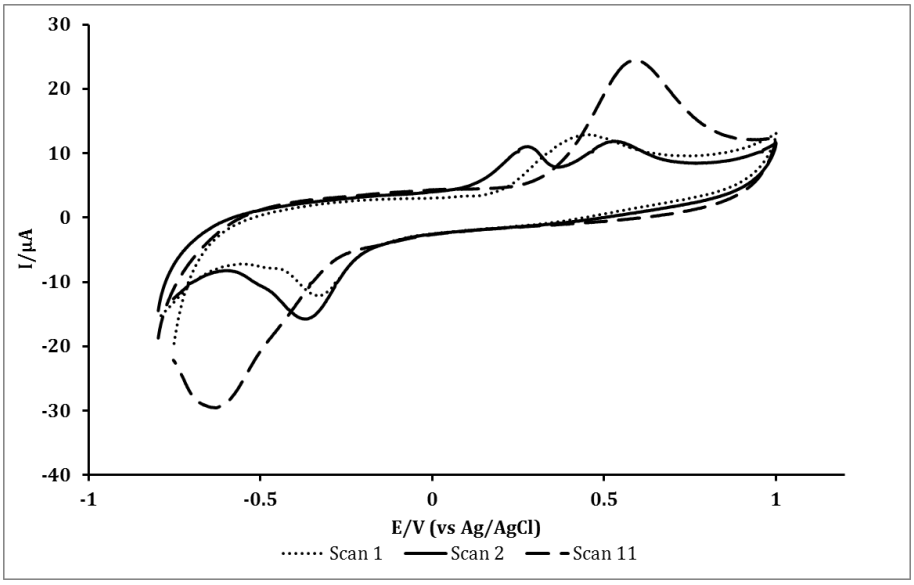

Fig. 4.6 CVs of the first (dotted), second (solid), and eleventh (dashed) cycles from Fig. 4.5.

A mechanism by which propofol radicals dimerise has been suggested by Heyne *et al*.[30] is given below in Fig. 4.7. The electron and proton transfer is believed to occur in a concerted manner.[31]

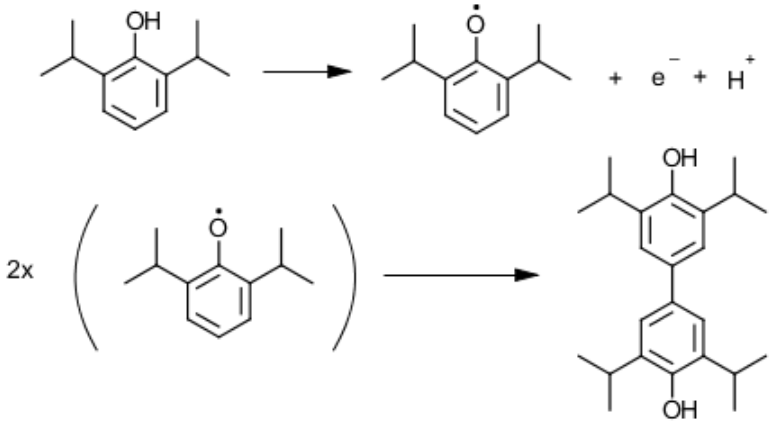

Fig. 4.7 Mechanism of propofol dimerisation.

The GCE was used to detect propofol quantitatively by chronoamperometry. The calibration plot in Fig. 4.8 below gives a detection limit of 14 μM and a sensitivity of 3.3×10^{-3} μA μM^{-1}.

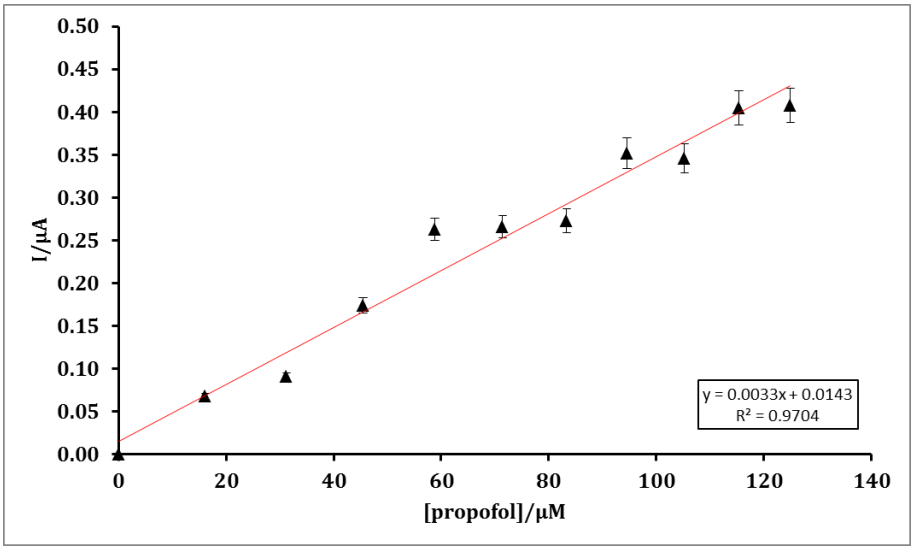

Fig. 4.8 Calibration plot for GCE used in amperometric mode. E=0.25 V. Background corrected. Error bars = ±5%

β-cyclodextrin modified GCE

GCEs modified with the hydrophobic cyclodextrins heptakis-(2,3,6-tri-O-acetyl)-β-cyclodextrin were briefly investigated. The hypothesis was that an electrode surface modified by cyclodextrins would be more selective to propofol and the cyclodextrins would reduce the interference of the signals associated with surface fouling. Fig. 4.9 demonstrates how this might be achieved. If the electrode surface were covered with adsorbed β-cyclodextrins, then access to the electrode surface would only be through the hydrophobic inner core of the cyclodextrins. Propofol fits inside this cavity,[32] and so the oxidised intermediate would be restricted from reacting with other propofol molecules.

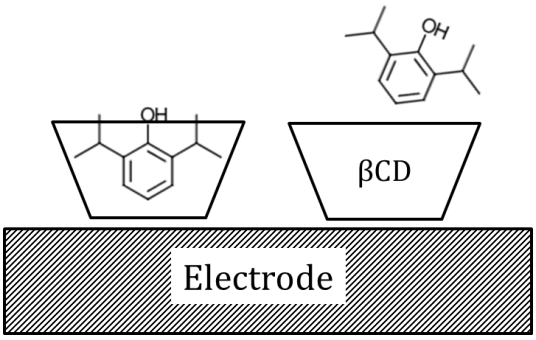

Fig. 4.9 Model showing how β-cyclodextrins can restrict access to the electrode surface.

A background scan in PBS from -0.4 V to 1.0 V (Fig. 4.10) showed that the β-cyclodextrin on the electrode surface has no significant interference on the measurements.

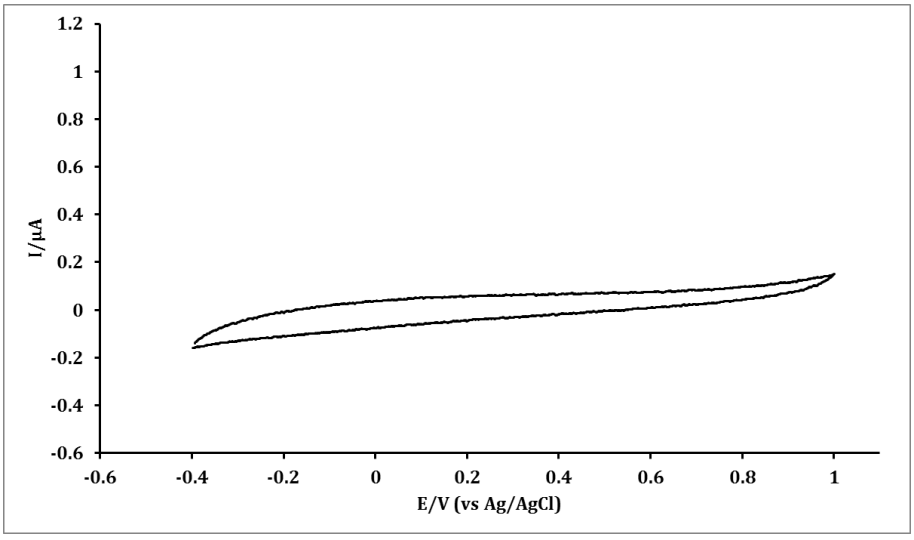

Fig. 4.10 CV of 0.1 M PBS by GCE modified with heptakis-(2,3,6-tri-O-acetyl)-β-cyclodextrin. Scan rate 10 mV s^{-1}.

When the modified GCE was introduced to a solution of propofol, CV gave different results compared to an unmodified GCE. These results are given in Fig. 4.11. On the first cycle, an oxidation peak at 0.4 V indicated the oxidation of propofol, as expected. However, upon continuous cycling, this peak reduced in current but a second peak corresponding to the oxidation of a polypropofol product, did not appear. The decrease in current corresponding to propofol oxidation with subsequent scans suggests that the

available concentration of propofol at the electrode surface decreases. This could be because as propofol is oxidised, it dimerises or polymerises, as per usual. As propofol is known to complex with β-cyclodextrins,[32] it can still be oxidised at the electrode surface, despite the presence of the β-cyclodextrin layer. However, the oxidation of this polypropofol product is not visible because the β-cyclodextrin discriminates against it based on size. This is due to the inclusion of propofol into the interior of the cyclodextrins cavity. Once could probably calculate the kinetics of the complexation, but fundamental studies were not part of the initial exploratory studies.

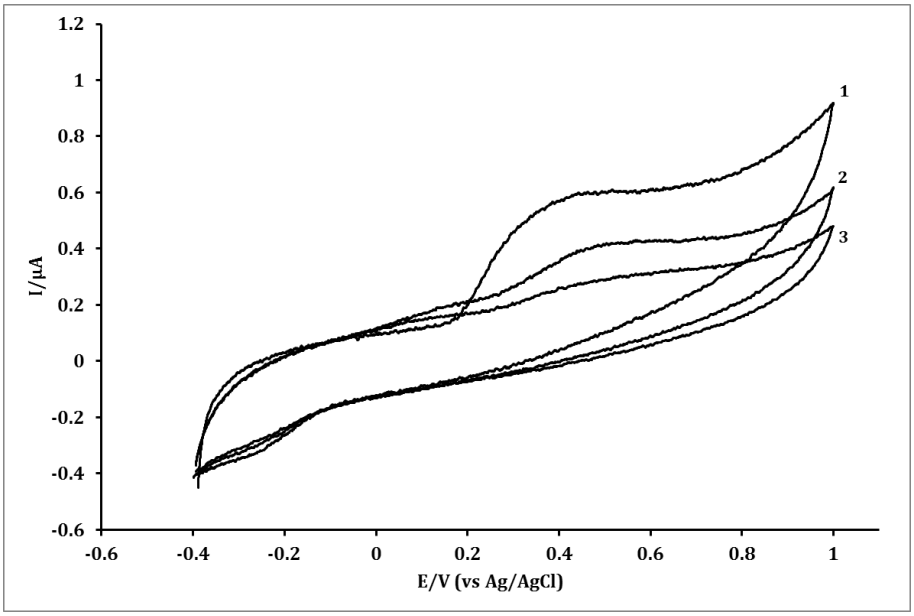

Fig. 4.11 CV of 500 μM propofol in PBS/ACN (90:10 v/v) by GCE modified with heptakis-(2,3,6-tri-O-acetyl)-β-cyclodextrin. Scan rate 10 mV s^{-1}. Cycles are indicated by numbers.

To test this theory, surface studies of the modified GCE surface would be necessary. Understanding the surface coverage and orientation of the β-cyclodextrin molecules would suggest whether this theory is reasonable. Alternatively, experiments where the cyclodextrin layer is tethered to the electrode surface, as in references 5 and 33, would ensure a consistent orientation.

CNT modified GCE

GCEs modified with MWNTs were investigated for propofol detection. It was found that the MWNT modification lowered the oxidation potential, but did not affect surface fouling. The oxidation overpotential was decreased to approximately 0.25 V (vs Ag/AgCl). The adsorption of the polypropofol product is evident in Fig. 4.12.

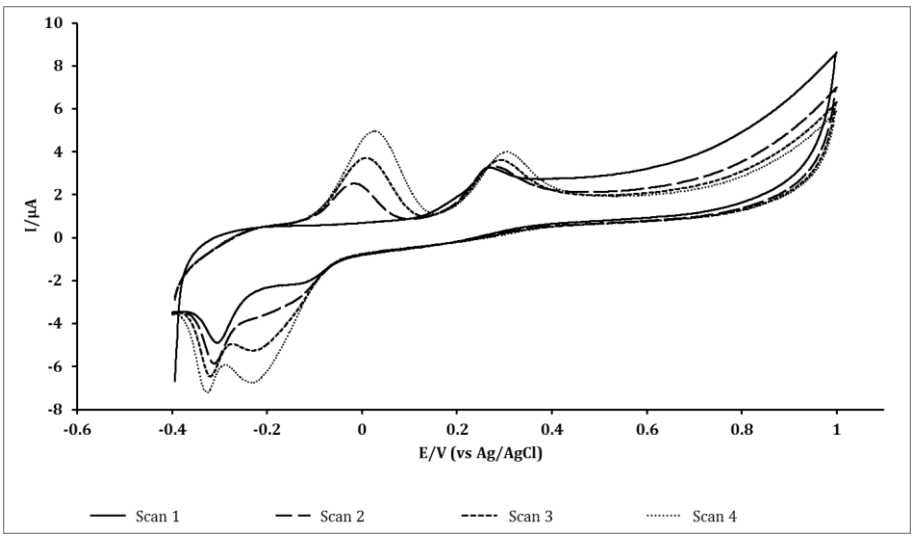

Fig. 4.12 CV of 500 μM propofol in PBS/ACN (90:10 v/v) by GCE modified MWNTs. Scan rate 10 mV s^{-1}.

A calibration plot for the MWNT modified GCE is given in Fig. 4.13. Although the MWNT modified GCE has a limit of detection of 18.9 μM, which is slightly higher than that of the bare GCE, it has a higher sensitivity than a bare GCE (1.02×10^{-2} μA μM^{-1} versus 3.3×10^{-3} μA μM^{-1}).

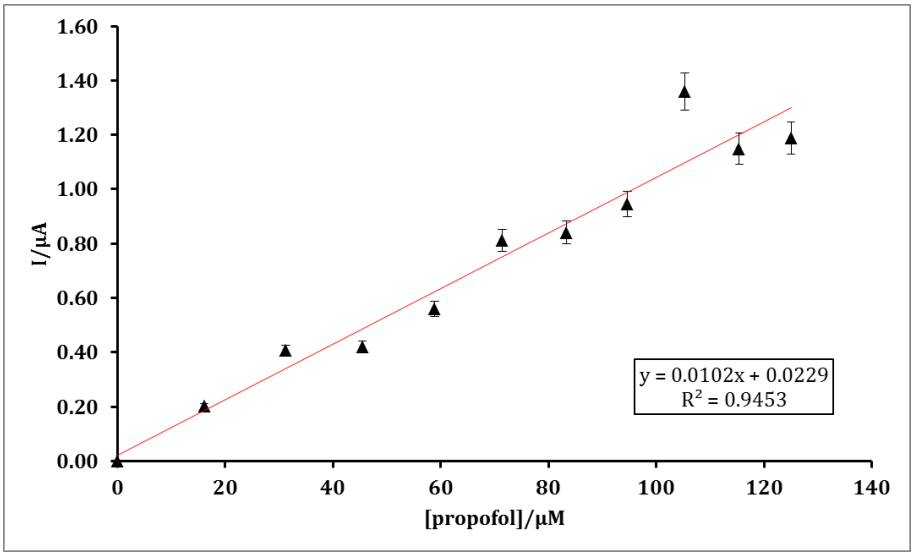

Fig. 4.13 Calibration plot for MWNT modified GCE used in amperometric mode. *E*=0.25 V. Background corrected. Error bars = ±5%

CNT paste electrodes

Because of the reported benefits of using CNTs to modify electrodes, namely decreases in oxidation overpotential[11] and surface fouling,[12] an electrode made out of CNTs was considered for propofol detection. A CV of the CNT paste electrode did not exhibit any oxidation or reduction of the MWNTs themselves and gave a relatively flat background. The background CV (Fig. 4.14) shows that there is a capacitve current of approximately 3.2 μA. This is considerably higher than that of the GCE (0.62 μA) and may be accounted for by the mineral oil used to bind the MWNTs.

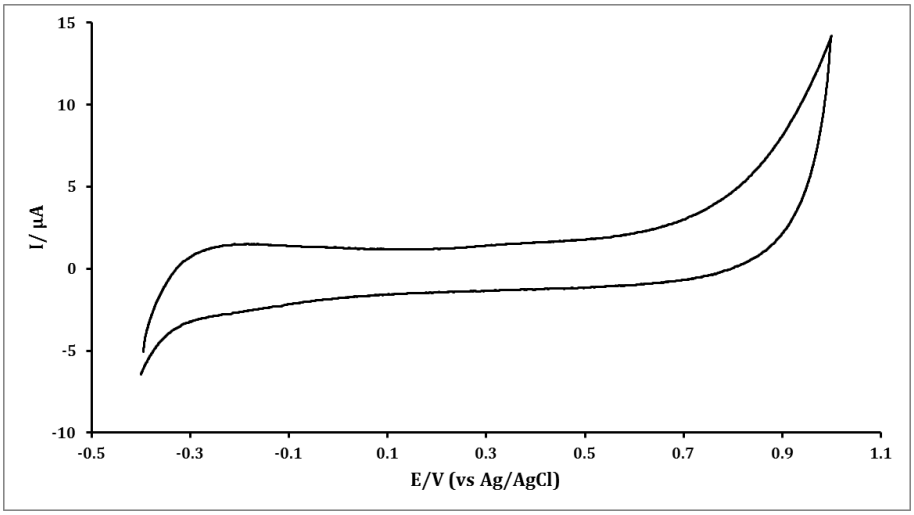

Fig. 4.14 CV of 0.1 M PBS with CNT paste electrode at 10 mV s^{-1}.

The CNT paste electrode also showed a good response with electroactive species. CV of 10 mM $K_3Fe(CN)_6$ (Fig. 4.15) shows reversible oxidation and reduction of $Fe^{2+/3+}$, with a difference in cathodic and anodic peak potentials of 80 mV.

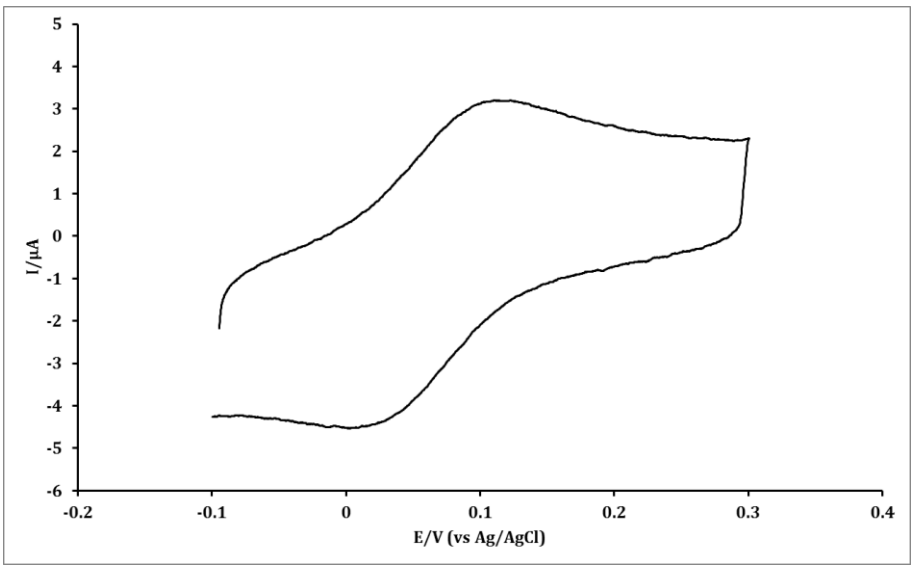

Fig. 4.15 CV of 10 mM $K_3Fe(CN)_6$ with CNT paste electrode at 10 mV s^{-1}.

When used to study propofol, the CNT paste electrode only displayed one of its two expected advantages. The oxidation potential was reduced to 0.25 V, compared to 0.5 V

for the GCE. From Fig. 4.16 it can be seen that product of propofol oxidation is still present and fouling occurs. This is likely due to only partial coverage of the electode surface by the CNTs.

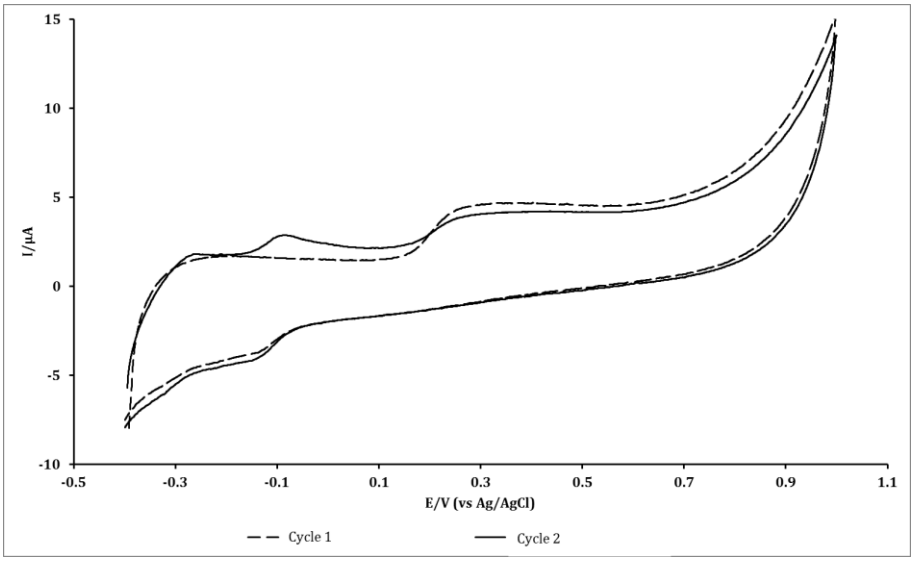

Fig. 4.16 CV of 50 µM propofol in PBS/ACN (90:10 v/v) at 10 mV s^{-1}. Cycle 2 (solid) shows the appearance of the polypropofol product.

Pre-anodised GCE

The pre-anodisation of GCEs was attempted in 0.5 M H_2SO_4 as reported by Thiagarajan *et al.*[7] It was reported that an increasing cathodic peak at 1.6 V (vs Ag/AgCl) was indicative of the pre-anodisation process. This was not evident in any electrode preparations, and so the method was abandoned. Pre-anodised GCEs have been reported elsewhere in the literature,[6,7,18] so the failure to achieve this was unusual.

Methylene Blue modified GCE

In the same way that polyMB has been shown to decrease the oxidation overpotential of NADH and reduce surface fouling,[25] the electropolymerisation of MB on a GCE was investigated to see if it might offer a similar catalytic advantage. First, exploratory

studies were conducted in solution. Fig. 4.17 shows the CV of a 50 μM solution MB at pH 7 in PBS in the potential range -0.7 to 0.8 V. Its oxidation and reduction is evident by the peak currents around -0.4 V. The low ΔE of the anodic and cathodic peaks (44.1 mV) suggests that there might be some adsorption to the electrode surface. The switching potential was kept below 1.0 V in order to avoid any electropolymerisation.

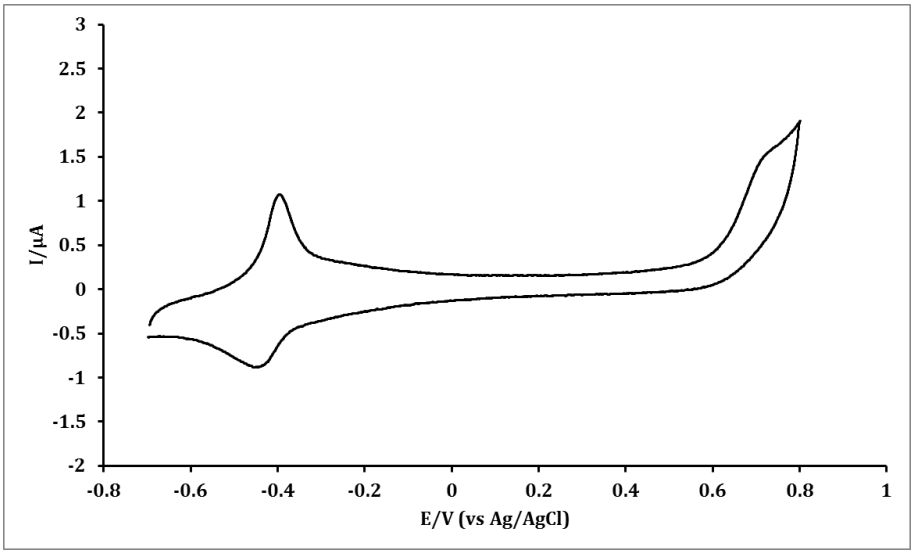

Fig. 4.17 CV of 50 μM MB in 0.1 M PBS, pH 7. Scan rate 10 mV s^{-1}.

Upon the introduction of 200 μM propofol (Fig. 4.18) to the system, peak currents are evident at 0.29 and -0.35 V (vs Ag/AgCl). This is a decrease in the oxidation potential by approximately 0.2 V compared to propofol electrooxidation at an unmodified GCE, and is similar to the effect of MB in other systems (*e.g.* NADH biosensors). This lowering of the oxidation potential is later maintained in the use of a polyMB film on a GCE (Fig. 4.20). Additionally, the anodic and cathodic peak potentials of MB appear to shift even closer together (15.9 mV).

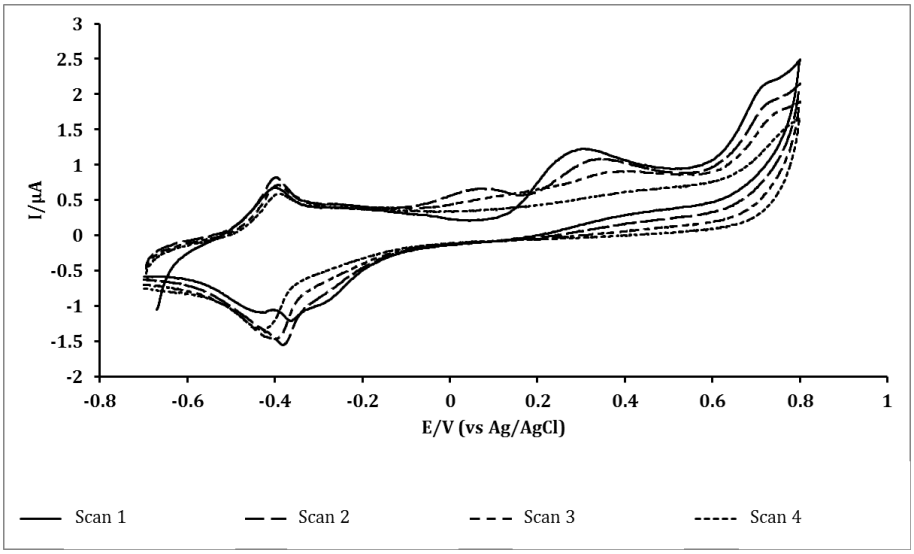

Fig. 4.18 CV of 200 µM propofol and 50 µM MB in 0.1 M PBS, pH 7. Scan rate 10 mV s^{-1}.

MB was next electropolymerised onto the surface of a GCE. The electropolymerisation is recorded in Fig. 4.19. Polymerisation of MB occurs best under basic conditions and the progressive increase in the redox couple peaks indicate that electropolymerisation has occurred.

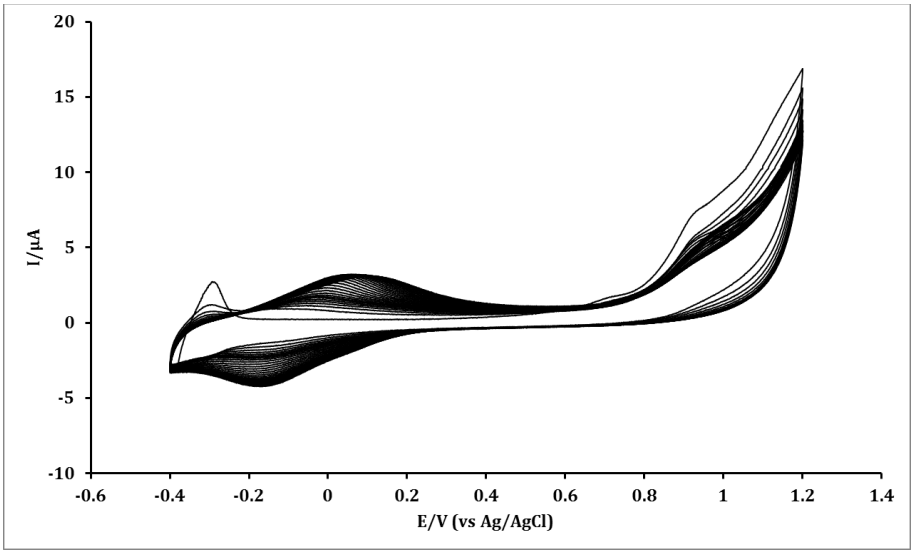

Fig. 4.19 Electropolymerisation of MB. 1 mM MB in 0.02 M borate buffer pH 9.08, 0.1 M KCl. 30 cycles. Scan rate 50 mV s^{-1}.

The effect of polyMB films on the electrochemical detection of propofol was next investigated. Fig. 4.20 compares background scans and CV in 200 μM solution of propofol. Only one scan is shown for each because subsequent scans were indistinguishable. The electrooxidation of propofol is indicated by an arrow in Fig. 4.20B. Only one peak was observed on the first and subsequent cycles, suggesting that the polypropofol product is either not formed or cannot be detected.

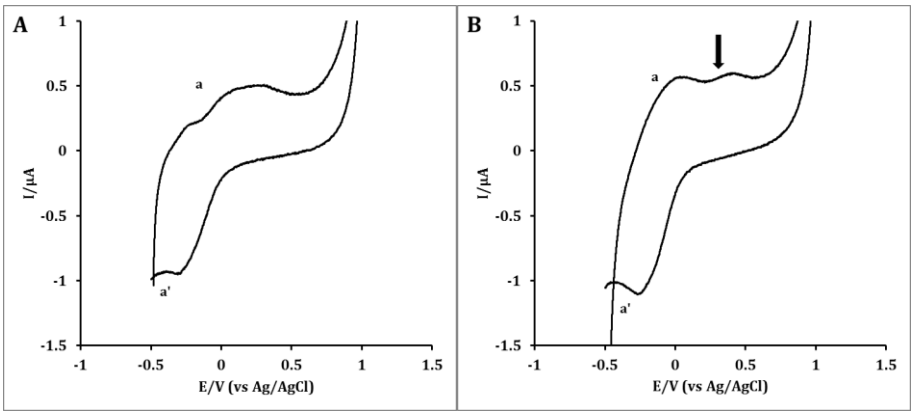

Fig. 4.20 CVs using a polyMB modified GCE. Both measurements taken in 0.1 M PBS pH 7 with **A** as a background and **B** in the presence of 200 μM propofol. Propofol oxidation is indicated by the arrow and a and a' indicate the anodic and cathodic currents of the polyMB film, respectively. Scan rate 10 mV s^{-1}.

CV conducted at pH 12 (*i.e.*, pH > pK_a) where propofol is easily ionisable, show a similar profile. From the CV in Fig. 4.21, the oxidation peaks of polyMB and propofol are the same as at a neutral pH. Additionally, the peak current for the oxidation of propofol continues to remain the same through progressive scans.

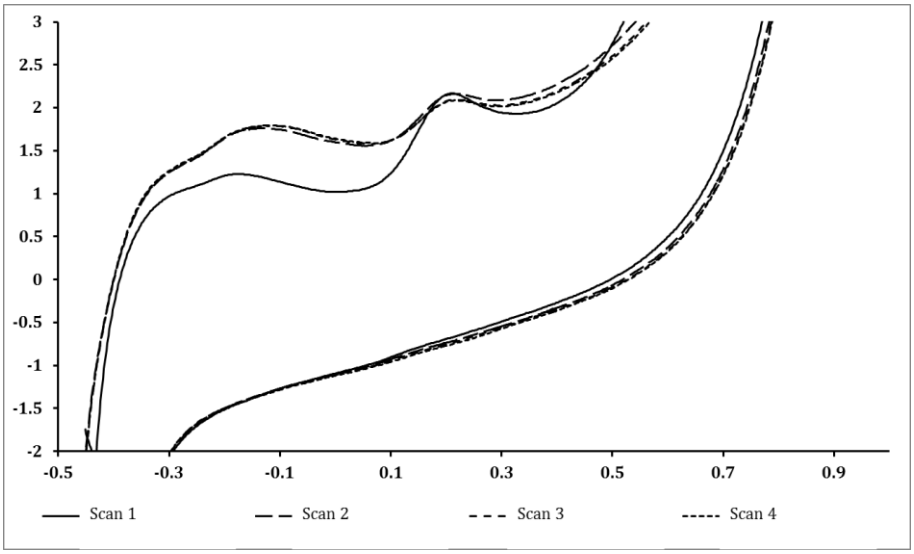

Fig. 4.21 CV of 100 μM propofol in borate buffer pH 12 with polyMB coated GCE. Scans 2-4 are almost indistinguishable. Scan rate 100 mV s^{-1}.

Amperometric measurements were made, but were not consistently reproducible, nor was any correlation between current and propofol concentration evident.

CONCLUSIONS

Many different modifications to the GCE were investigated. Calibration curves and limits of detection were calculated for two methods—an unmodified GCE and a GCE with MWNTs adsorbed to the surface. It was found that the MWNT coating did not increase the detection limit for propofol, but greatly increased the electrode's sensitivity.

PolyMB coated GCEs did, however, show a decrease in electrode fouling by the polypropofol product as did those coated with β-cyclodextrin. This is advantageous because it means that electrodes can be reused, rather than having to be replenished from measurement to measurement. The β-cyclodextrin coated electrode, however, exhibited a decrease in propofol oxidation current with progressive cycles of CV.

As the MWNT coated GCEs showed the highest sensitivity and all the modifications that were tested quantitatively had detection limits of the same order, MWNT coated GCEs should be further developed and studied for their use as electrochemical sensors for propofol.

REFERENCES

(1) Durst, R. A.; Baumner, A. J.; Murray, R. W.; Buck, R. P.; Andrieux, C. P. *Pure Appl. Chem.* **1997**, *69*, 1317.

(2) Heald, C. G. R.; Wildgoose, G. G.; Jiang, L.; Jones, T. G. J.; Compton, R. G. *ChemPhysChem* **2004**, *5*, 1794.

(3) Fleischmann, M.; Hendra, P. J.; McQuillan, A. J. *Chem. Phys. Lett.* **1974**, *26*, 163.

(4) Uosaki, K.; Sato, Y.; Kita, H. *Langmuir* **1991**, *7*, 1510.

(5) Grancharov, G.; Khosravi, E.; Wood, D.; Turton, A.; Kataky, R. *Analyst* **2005**, *130*, 1351.

(6) Engstrom, R. C. *Anal. Chem.* **1982**, *54*, 2310.

(7) Thiagarajan, S.; Cheng, C.-Y.; Chen, S.-M.; Tsai, T.-H. *J. Solid State Electr.* **2011**, *15*, 781.

(8) Iijima, S. *Nature* **1991**, *354*, 56.

(9) Banks, C. E.; Davies, T. J.; Wildgoose, G. G.; Compton, R. G. *Chem. Commun.* **2005**, 829.

(10) Wang, J. *Electroanal.* **2005**, *17*, 7.

(11) Wu, K. B.; Fei, J. J.; Hu, S. S. *Anal. Biochem.* **2003**, *318*, 100.

(12) Musameh, M.; Wang, J.; Merkoci, A.; Lin, Y. *Electrochem. Comm.* **2002**, *4*, 743.

(13) Banks, C. E.; Compton, R. G. *Analyst* **2005**, *130*, 1232.

(14) Scipioni, R.; Pumera, M.; Boero, M.; Miyahara, Y.; Ohno, T. *The Journal of Physical Chemistry Letters* **2009**, *1*, 122.

(15) Valentini, F.; Amine, A.; Orlanducci, S.; Terranova, M. L.; Palleschi, G. *Anal. Chem.* **2003**, *75*, 5413.

(16) Ferancova, A.; Labuda, J. *Fresen. J. Anal. Chem.* **2001**, *370*, 1.

(17) Rojas, M. T.; Koniger, R.; Stoddart, J. F.; Kaifer, A. E. *J. Am. Chem. Soc.* **1995**, *117*, 336.

(18) Engström, R. C.; Strasser, V. A. *Anal. Chem.* **1984**, *56*, 136.

(19) Cabaniss, G. E.; Diamantis, A. A.; Murphy, W. R.; Linton, R. W.; Meyer, T. J. *J. Am. Chem. Soc.* **1985**, *107*, 1845.

(20) Magne, P.; Walker, P. L. *Carbon* **1986**, *24*, 101.

(21) Mahajan, O. P.; Morenocastilla, C.; Walker, P. L. *Separ. Sci. Technol.* **1980**, *15*, 1733.

(22) Mahajan, O. P.; Morenocastilla, C.; Walker, P. L. *Carbon* **1980**, *18*, 47.

(23) Chen, P.; McCreery, R. L. *Anal. Chem.* **1996**, *68*, 3958.

(24) Karyakin, A. A.; Strakhova, A. K.; Karyakina, E. E.; Varfolomeyev, S. D.; Yatsimirsky, A. K. *Bioelectroch. Bioener.* **1993**, *32*, 35.

(25) Karyakin, A. A.; Karyakina, E. E.; Schuhmann, W.; Schmidt, H.-L.; Varfolomeyev, S. D. *Electroanal.* **1994**, *6*, 821.

(26) Karyakin, A. A.; Karyakina, E. E.; Schuhmann, W.; Schmidt, H.-L. *Electroanal.* **1999**, *11*, 553.

(27) Silber, A.; Hampp, N.; Schuhmann, W. *Biosens. Bioelectron.* **1996**, *11*, 215.

(28) Elving, P. J.; Bresnahan, W. T.; Moiroux, J.; Samec, Z. *Bioelectroch. Bioener.* **1982**, *9*, 365.

(29) Bard, A. J.; Faulkner, L. R. *Electrochemical Methods: Fundamentals and Applications*; John Wiley & Sons, Inc.: New York, 2001.

(30) Heyne, B.; Tfibel, F.; Hoebeke, M.; Hans, P.; Maurel, V.; Fontaine-Aupart, M.-P. *Photochem. Photobiol. Sci.* **2006**, *5*, 1059.

(31) Costentin, C.; Louault, C.; Robert, M.; Savéant, J.-M. *PNAS* **2009**, *106*, 18143.

(32) Trapani, G.; Latrofa, A.; Franco, M.; Lopedota, A.; Sanna, E.; Liso, G. *J. Pharm. Sci.* **1998**, *87*, 514.

(31) Nelles, G.; Weisser, M.; Back, R.; Wohlfart, P.; Wenz, G.; MittlerNeher, S. *J. Am. Chem. Soc.* **1996**, *118*, 5039.

CHAPTER 5 : CONCLUSIONS & FUTURE WORK

The aim of the project was to develop an electrochemical sensor for propofol that would be optimal for point of care testing. While this initial aim was not realised, many different approaches to the electrochemical detection of propofol were explored. These include the use of facilitated transfer at the μITIES and the use of modified GCEs.

Of all the methods employed, detection of propofol by facilitate transfer at the μITIES was the most complicated but also the most interesting means of detecting and quantifying propofol. More experimentation and research in this area should be conducted as it is the first time a charged carrier was used with a μITIES setup to detect a neutral molecule.

The most promising detection methods were those where modifications to a GCE were made. Modifiying GCEs with MWNTs proved to be the most effective modification, however it did not appropriately deal with the effects of electrode fouling. Perhaps a combination of methods would prove to make an ideal sensor. There are reports in the literature of MWNT based electrodes that have been modified with redox dyes that show reduced electrode surface fouling.[1,2]

REFERENCES

(1) Zou, Y. J.; Sun, L. X.; Xu, F. *Talanta* **2007**, *72*, 437.

(2) Umasankar, Y.; Periasamy, A. P.; Chen, S. M. *Anal. Biochem.* **2011**, *411*, 71.

APPENDIX I

Attended Talks & Summaries

Synthetic Biology to Interface Cells with Machines and Materials
Daniel Frankel, Newcastle University

The main thrust of Dr Frankel's talk was centred on what he refers to as "cyberplasm"—hybrid bio/machine robots. This was a captivating talk which looked specifically at a collaborative project where his team are working to develop a "synthetic lamprey". This system was chosen because it is very simple, essentially consisting of a head that senses and controls connected to a body that moves the "creature".

The challenges associated with trying to develop this bio/machine hybrid are numerous. The one specific aspect Frankel has chosen to focus on is sensing. The ability to chemically sense the environment and then relay that as an electrical signal is vital for any autonomous bio-hybrid device. The way in which Frankel chose to attack this problem was quite interesting. The general strategy employed relies on using receptors on a biological cell that are specific for the analyte of interest. This results in a signal cascade within the cell that can be programmed through genetic engineering to produce a desired result. One example is the production of a chemical that is secreted and can then be electrochemically detected outside the cell. In this step, the signal is converted from its chemical and biological nature to an electrical signal.

On the whole, the Cyberplasm project appears to be "fairytale science" with significant wow-factor and little realisation. However, to its credit, the problems associated with this project are valuable contributions to science and technology. In particular, getting biology to interface with machines may have a host of applications.

Green Chemistry and Supercritical Fluids
Prof. Martyn Poliakoff

Green chemistry is a growing field mainly focused on process development improvements that minimise the environmental impact of large scale chemical syntheses. A large portion of research in this area investigates using supercritical CO_2 to replace environmentally hazardous organic solvents. A major advantage of chemistry in supercritical fluids is the ease of separation of the product from the solvent. Separation simply involves decreasing the pressure and the gaseous solvent evaporates from the product. The gaseous solvent can then be returned to the reaction chamber and reused.

Supercritical fluids are simply gases that exist beyond the critical point (as determined by temperature and pressure) and combine the properties of gases and liquids. Work in Prof. Poliakoff's group focuses on continuous reactions with on-line analysis and covers various areas including hydrogenation, acid catalysis, and photo-oxidation.

Hydrogenation reactions in $scCO_2$ have gone from the simple hydrogenation of cyclohexene to more complex reactions such as the hydrogenation of isophorone over a palladium catalyst to trimethylcyclohexanone. It was the latter reaction that was researched in conjunction with and implemented by Thomas Swan & Co. The challenge with this reaction was the possibility of the production of over-hydrogenated by-products.

Solid acid catalysis is another area of research within Prof Poliakoff's group and a significant amount of work is focused on the dehydration of alcohols to form ethers. Photo-oxidation was another interesting area of research. The advantage that supercritical fluids offer in this area is that $^1O_2$ has a longer lifetime in $scCO_2$.

All Departmental Seminars attended

Dr Karen Edler	*Mesostructured Polymer-Surfactant Films*	27/10/10
Prof Martyn Twigg	*Controlling Emissions From Cars*	10/11/10
Dr Ed Tate	*Getting a Chemical Handle on Protein Modification*	8/12/10
Prof Andrew de Mello	*High-Throughput Chemistry & Biology*	19/01/11
Dr Andrew Goodwin	*Local Structure & Dynamics in Functional Framework Materials*	26/01/11
Prof Franstisck Hartl	*Spectroelectrochemical Studies of CO_2 reducing systems*	2/02/11
Prof Martyn Poliakoff	*Green Chemistry & Supercritical Fluids*	23/02/11
Prof Joachim Spatz	*Cellular Response at the Nanoscale*	3/03/11
Dr Daniel Frankel	*Synthetic Biology to Interface Cells with Machines and Materials*	03/03/11
Prof Molly Stevens	*Bio-Inspired Materials for Regenerative Medicine and Biosensing*	03/03/11
Prof Neil Champness	*Molecular Organisation: Working with Molecules on the Nanoscale*	09/03/11